Supporting information

An organometallic complex formed by an unconventional radical SAM enzyme

Min Dong, [1,#] Masaki Horitani, [2,#] Boris Dzikovski,[1] Maria-Eirini Pandelia[3], Carsten Krebs[4], Jack H. Freed,[1] Brian M. Hoffman[2,*] and Hening Lin[1,5,*]

[1]Department of Chemistry and Chemical Biology, Cornell University, Ithaca, New York, 14853. [2]Department of Chemistry, Northwestern University, Evanston, Illinois 60208. [3]Department of Biochemistry, Brandeis University, MA 02453. [4]Department of Chemistry and Department of Biochemistry and Molecular Biology, The Pennsylvania State University, University Park, Pennsylvania 16802. [5]Howard Hughes Medical Institute, Cornell University, Ithaca, New York, 14853.

A. Reagents and Methods **S2-S9**
B. Supplementary Figures **S10-S32**
C. References **S33**

A. Reagents and Methods

General methods. The reagents for organic synthesis were purchased from Sigma-Aldrich or TCI. ^{1}H and ^{13}C-NMR were performed on INOVA 400 and 600 MHz spectrometers. LCMS was carried out on a SHIMADZU HPLC and Thermo LCQ FLEET mass spectrometer with a Sprite TARGA C18 column (40 × 2.1 mm, 5 μm, Higgins Analytical, Inc.) monitoring at 215 and 254 nm. Solvents used in LCMS for positive mode were water with 0.1% acetic acid and acetonitrile with 0.1% acetic acid, and for negative mode were water and acetonitrile. Mobile phases used for analytic and preparative HPLC were 0.1% aqueous TFA (solvent A) and 0.1% TFA in acetonitrile (solvent B). Analytic HPLC analysis was performed using Kinetex 2.6 μm XB-C18 100×4.6 mm column with UV detection at 215 nm and 254 nm. Preparative HPLC purification was carried out using Targa^{TM} Prep C18 10μm 250×20mm reverse phase column with UV detection at 215 nm and 254 nm. Protein purification, enzymatic reactions and sample preparation for EPR were performed in an anaerobic chamber (Coy Laboratory Products). X band EPR spectra were recorded at ACERT on a Bruker ElexSys E500 EPR spectrometer at a frequency of 9.25 GHz in quartz tubes with internal diameters of 4 mm. EPR measurements at 12K and 30 K were carried out using an ESR910 liquid-helium cryostat (Oxford Instruments). The spectrometer settings were as follow if without specific note: modulation frequency, 100 kHz; modulation amplitude, 8 G; microwave power, 0.63 mW. The field sweeps were calibrated with a BRUKER ER 035 Gauss meter and the microwave frequency was monitored with a frequency counter. Data acquisition and manipulation were performed with Xepr software. Q-band CW EPR and ENDOR spectra were collected on a spectrometer with a helium immersion dewar previously reported.[1,2] All Q-band CW EPR and ENDOR measurements were done at 2 K.

Synthesis of SAM_{CA}

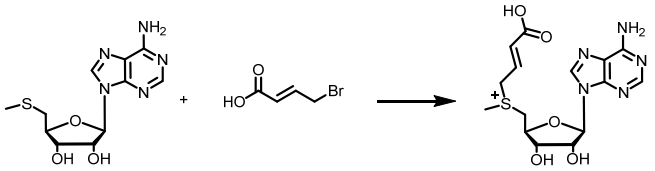

S1 S2 SAM_{CA}

The synthetic method used was similar to that reported for synthesizing other SAM analogues[3] with slight modification. 4-Bromocrotonic acid (45 mg, 270 μmol) was dissolved in acetic acid (100 μL) and formic acid (100 μL). 5'-Deoxy-5'-methylthioadenosine (MTA) (8 mg, 27 μmol) was added at 0℃. $AgClO_4$ (24 mg, 108 μmol) was dissolved in 50 μl acetic acid and then added to the previous solution at 0℃. This mixture was stirred for 20 min at 0℃ and then for additional 5 h at room temperature. After diluted with 3 mL of cold water, the reaction was filtered to remove the precipitated AgBr. The diluted filtrate was loaded onto preparative HPLC for purification. SAM_{CA} was eluted at 23 min with a flow rate of 10 mL/min with the following gradient: 0% solvent B for 20 min, then 0 % to 40% solvent B over 40 min. Freeze drying of the HPLC fractions yielded SAM_{CA} as a white powder (9 mg, 87% yield, 3:2 mixture of stereoisomers). ^{1}H NMR (400 MHz, D_2O) δ 8.27(s, 1H, H-8),8.26 (s, 1H, H-2), 6.44-6.58(m, 1H, CH_2-CH=), 6.0-6.01(d, 1H, H-1′), 5.81-6.0 (dd, 1H, J=60, 16, =CH-COO^-), 4.65-4.72 (m, 1H, H-2′), 4.49-4.56 (m, 1H, H-3′), 4.36-4.45 (m, 1H, H-4′), 4.03-4.07 (m, 2H, S-CH_2), 3.66-3.76 (m, 2H, H-5′), 2.78, 2.80 (d, 3H, S-Me). ^{13}C NMR (125 MHz, D_2O) δ 168.1, 168.0, 163.0, 162.8, 150.2, 147.9, 144.7, 143.6, 143.5, 132.4, 132.0, 131.6, 131.4, 119.4, 117.5, 115.1, 90.3, 90.1, 79.0, 78.5, 73.2, 72.9, 72.8, 72.6, 42.8, 42.5, 41.5, 22.7, 22.5. LCMS (ESI) calcd. for $C_{15}H_{20}N_5O_5S$ $[M]^+$ 382.1, obsd. 382.2.

Analysis of the products of the enzymatic reactions of PhDph2 and SAM_{CA} by high-

performance liquid chromatography (HPLC). The PhDph2 protein used here was expressed and purified as reported previously[4]. The reactions were set up under anaerobic condition. The full reaction contained 30 μM PhDph2, 10 mM dithionite, 60 μM SAM_{CA}, 150 mM NaCl, 1 mM DTT and 200 mM Tris-HCl at pH 7.4 in a final volume of 30 μL. The control samples (without PhDph2, dithionite, or SAM_{CA}) were set up similarly by replacing the corresponding component with equal volume of water respectively. The reactions were incubated at room temperature for 20 min and quenched by adding 30 μL of 10% TFA in water. Protein was precipitated by centrifugation and the supernatant was applied to HPLC and resolved with a linear gradient of 0 to 40% buffer B over 15 min at a flow rate of 0.5 mL/min.

The time dependent experiments were set up as described below in EPR experiment. A total volume of 40ul reaction was set up, 6ul aliquot of which was quenched by 54 μL of 10% TFA at different time points: 0 sec, 10 sec, 30 sec, 5 min, 10 min and 15 min. Then Protein was spun down and the supernatant was analyzed by HPLC.

Sample preparation for EPR experiments. A complete reaction (700 μM PhDph2, 1 mM dithionite, and 5 mM SAM_{CA} in 100 μL of 100 mM phosphate buffer with 150 mM sodium chloride, pH 7.4) and controls (without PhDph2 or dithionite) were set up in an anaerobic chamber. The reactions were transferred to EPR tubes in 30 sec after set up, frozen in liquid N_2 and sealed in the anaerobic chamber and then taken out for EPR analysis. The EPR experiments for SAM and aza-SAM_{CA} were set up as above.

The time dependent experiments (700 μM PhDph2, 10 mM dithionite, and 5 mM SAM_{CA} in 100 mM phosphate buffer with 150 mM sodium chloride, pH 7.4) were set up with the volume of 60ul for each time point. The reactions were transferred to EPR tubes and frozen in liquid N_2 at different time points: 2 sec, 30 sec, 2 min, 5 min and 15 min. Then the tubes were sealed in the anaerobic chamber and taken out for EPR analysis.

For the redox experiments of CA in Figure S25, dithionite(10mM) or $K_3[Fe(CN)_6]$ (5mM) was added to the samples set up as above. EPR spectra were recorded before and after adding the reductant or oxidant.

Sample preparation for ^{1}H-NMR and ^{1}H/^{13}C HMBC NMR to detect reaction products.

A complete reaction (400 μM PhDph2, 10 mM dithionite, and 4 mM SAM_{CA} in 50 μL of 100 mM phosphate buffer with 150 mM sodium chloride, pH 7.4) and controls (without PhDph2 or dithionite) were set up in an anaerobic chamber. The samples were incubated for 2 hr at room temperature. D_2O (300 μL) was added to each sample and the solution was transferred to a Millipore Microcon YM-10 filter unit. The filtrate was transferred to a Shigemi D_2O-matched NMR tube and directly applied to NMR experiments. The spectrum for the standard compound crotonic acid was obtained in 100 mM phosphate buffer pH 7.4. For ^{1}H/^{13}C HMBC experiment, the reaction was set up with the volume scaled up to 400ul. After incubation, 30ul D_2O was added. The mixture was treated as described above. ^{1}H-NMR and HMBC spectra were obtained on an INOVA 600 spectrometer.

Sample preparation for ENDOR experiments.

The procedure of sample preparation for ENDOR experiments was similar to that for EPR, except the phosphate buffer was replaced by 200 mM Tris-HCl buffer with 150 mM sodium chloride, pH 7.4.

Synthesis of Aza-SAM_{CA}

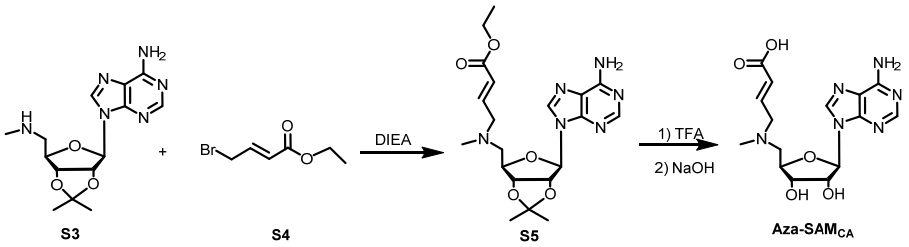

4-Bromide-ethyl crotonate (36 mg, 187 µmol) and 5'-deoxy-5'-(methylamino)- 2',3'-O-isopropylidene-adenosine (50 mg, 156 µmol) were dissolved in 2 mL of acetonitrile. *N*,*N*-Diisopropylethylamine (64µL, 374 µmol) was added to the reaction. The mixture was stirred at 70℃ for 12 hr. The solvent was removed under vacuum. The residue was applied to preparative HPLC. Compound **S5** was eluted at 34 min with a flow rate of 10 mL/min with the following gradient: 0% solvent B for 10 min, then 0% to 60% solvent B over 50 min. Compound **S5** was obtained in 38% yield (30 mg). Compound **S5** (5 mg, 11.6 µmol) was dissolved in 1 mL of 90% trifluoroacetic acid solution. The mixture was stirred for 0.5 hr at room temperature. Then the reaction was evaporated in vacuum. This residue was dissolved in 2 mL of 1 M NaOH solution. The reaction was stirred at room temperature for 1 hr and neutralized by 6 M HCl. The solution was directly applied to HPLC. Aza-SAM$_{CA}$ was eluted at 12 min with a flow rate of 10 mL/min with the following gradient: 0% solvent B for 10 min, then 0 % to 40 % solvent B over 50 min. The product was obtained in 80% yield (3.3 mg). ^{1}H-NMR (400 MHz, D_2O) δ 8.27 (s, 1H), 8.26 (s, 1H), 6.56 (m, 1H), 6.01 (d, J = 4.2 Hz, 1H), 5.98 (d, J =14.8 Hz, 1H), 4.72 (m, 1H), 4.44-4.36 (m, 2H), 3.96-3.86 (m, 2H), 3.65 (m, 1H), 3.46 (m, 1H), 2.82 (s, 3H). LCMS (ESI) calcd. for $C_{15}H_{21}N_6O_5$ $[M+H]^+$ 365.2, obsd. 365.2.

Synthesis of isotope labeled SAM$_{CA}$

Synthesis of 3-^{13}C SAM$_{CA}$

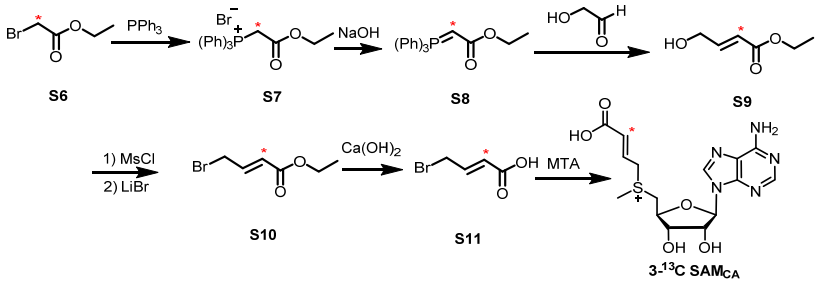

[2-^{13}C](Ethoxycarbonylmethyl)triphenylphosphonium Bromide (S7)

Ethyl [2-^{13}C]-2-bromoacetate (50 mg, 0.3 mmol) in ethyl acetate (1 mL) was added to a solution of triphenylphosphine (81 mg, 0.31 mmol) in ethyl acetate (1 mL). The reaction mixture was stirred at room temperature for 12 h. The white precipitate was filtered off, washed with diethyl ether (3 × 1 mL), and dried under vacuum to give **S7** (118 mg, 92% yield). ^{1}H NMR (400 MHz, $CDCl_3$) δ 7.79 – 7.70 (m, 6H), 7.69 – 7.63 (m, 3H), 7.59 – 7.50 (m, 6H), 5.46 (d, J = 13.9 Hz, 1H), 5.12 (d, J = 13.9 Hz, 1H), 3.86 (q, J = 7.1 Hz, 2H), 0.89 (t, J = 7.1 Hz, 3H).

[2-^{13}C](Ethoxycarbonylmethylene)triphenylphosphorane (S8)

Sodium hydroxide (1.0 M, 1 mL) solution was added to a solution of S7 (128 mg, 298 µ mol) in DCM (1 mL). The reaction mixture was stirred vigorously for 15 min. The organic layer was separated and the aqueous layer extracted with DCM (3 × 1 mL). The combined organic layers were dried over Na_2SO_4 and concentrated under vacuum to give **S8** (103 mg, 99% yield). ^{1}H NMR (400

MHz, $CDCl_3$) δ 7.37–7.65 (m, 15H), 3.92 (br, 2H), 2.84 (br, 1H), 1.06 (br, 3H).

[2-^{13}C]4-Hydroxyl-ethyl crotonate (S9)

To a suspension of glycolaldehyde dimer (40 mg, 0.33 mmol) in H_2O (2 mL) was added [2-^{13}C]-(ethoxycarbonylmethylene)triphenylphosphorane (103 mg, 0.3 mmol). The mixture was stirred for 12 h at room temperature. The reaction was filtered. Filtrate was extracted by ethyl acetate (3 × 3 mL). The combined organic layers were dried over anhydrous Na_2SO_4. The solvent was evaporated in vacuum and the crude product was purified by silica gel column chromatography (hexane:ethyl acetate 5:1) to give **S9** (28 mg, 72% yield). ^{1}H NMR (400 MHz, $CDCl_3$) δ 6.56 – 6.33 (m, 1H), 6.06 (d, *J* = 11.8, 0.5H), 5.65 (d, *J* = 11.8, 0.5H), 4.56 (t, *J* = 5.3 Hz, 2H), 4.18 (q, *J* = 7.2 Hz, 2H), 3.09 (s, 1H), 1.28 (t, *J* = 7.2 Hz, 3H).

[2-^{13} C]4-bromide ethyl crotonate (S10)

4-hydroxyl ethyl crotonate (28 mg, 0.22mmol) was dissolved in DCM (2 mL). The solution was cooled to 0℃. Methanesulfonyl chloride (51μl, 0.66mmol) and triethylamine (107μL, 0.77 mmol) were added consequently at 0℃. The mixture was stirred at room temperature for 2 hr. The reaction was quenched by iced H_2O (3 mL) and extracted with ether (3 × 5 mL). The combined organic layers were dried over Na_2SO_4 and the solvents were evaporated under vacuum. This residue was dissolved in acetone (2 mL). Lithium bromide (48 mg 0.55 mmol) in 0.5 mL of acetone was added to the reaction. The mixture was stirred overnight. The solvent was evaporated under vacuum and the crude product was purified by silica gel column chromatography (hexane:ethyl acetate 25:1) to give **S10** (27 mg, 63% yield). ^{1}H NMR (400 MHz, $CDCl_3$) δ 6.99 (dd, *J* = 15.3, 1.9 Hz, 1H), 6.21 (d, *J* = 15.3 Hz, 0.5H), 5.80 (d, *J* = 15.3 Hz, 0.5H), 4.20 (q, *J* = 7.1 Hz, 2H), 3.99 (ddd, *J* = 7.3, 5.9, 1.2 Hz, 2H), 1.28 (t, *J* = 7.1 Hz, 3H).

[2-^{13}C]4-bromide-crotonic acid (S11)

4-bromide ethyl crotonate (27 mg, 0.14 mmol) was dissolved in ethanol (1 mL). Then H_2O (2 mL) and calcium hydroxide (21 mg, 0.28 mmol) were added. The mixture was stirred at room temperature for 5 hr. The reaction was neutralized by 1 N HCl at 0℃. Ethanol was evaporated under vacuum and the aqueous solution was extracted by ethyl acetate (3 × 5 mL). The combined organic layers were dried over Na_2SO_4 and concentrated under vacuum to give **S11** (22 mg, 95% yield). ^{1}H NMR (400 MHz, $CDCl_3$) δ 7.10 (dtd, *J* = 15.3, 7.3, 1.9 Hz, 1H), 6.24 (dt, *J* = 15.3, 1.3 Hz, 0.5H), 5.82 (dt, *J* = 15.3, 1.3 Hz, 0.5H), 4.09 – 3.93 (m, 2H)

3-^{13}C SAM_{CA}

3-^{13}C SAM_{CA} was synthesized with [2-^{13}C] 4-bromide-crotonic acid and MTA according to the same procedure for the synthesis of SAM_{CA}.

3-^{13}C SAM_{CA} (3:2 mixture of stereoisomers). ^{1}H NMR (400 MHz, D_2O) δ 8.27(s, 1H), 8.25 (s, 1H), 6.60 – 6.38 (m, 1H), 6.10 (dd, *J* = 59.6, 16.4 Hz, 0.5H), 5.99 (d, *J* = 3.6 Hz, 1H), 5.69 (dd, *J* = 59.6, 16.4 Hz, 0.5H), 4.68 (m, 1H), 4.52 (dt, *J* = 17.3, 5.9 Hz, 1H), 4.45 – 4.34 (m, 1H), 4.10 – 3.98 (m, 2H), 3.79 – 3.63 (m, 2H), 2.78 (s, s, 3H). LCMS (ESI) calcd. for $C_{15}H_{20}N_5O_5S$ $[M]^+$ 383.1, obsd. 383.0.

Synthesis of 2-^{13}C SAM_{CA}

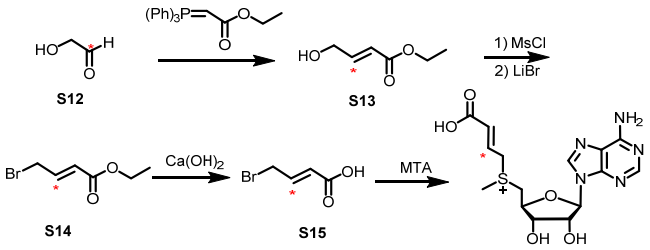

2-^{13}C SAM$_{CA}$ was synthesized according to the same procedure for the synthesis of 3-^{13}C SAM$_{CA}$ by employing [1-^{13}C] glycolaldehyde, starting from the **S9** preparation step.

2-^{13}C SAM$_{CA}$ (3:2 mixture of stereoisomers) ^{1}H NMR (400 MHz, D_2O) δ 8.25 (d, 1H), 8.24 (d, 1H), 6.77 – 6.54 (m, 0.5H), 6.35 – 6.14 (m, 0.5H), 5.99 (d, 1H), 5.97 (d, J = 15.2 Hz, 0.4H), 5.83 (d, J = 15.2 Hz 0.6H), 4.72-4.65 (m, 1H), 4.54 (t, J = 6.0 Hz, 0.6H), 4.50 (t, J = 6.0 Hz, 0.4H), 4.44-4.35 (m, 1H), 4.08-4.01(m, 2H), 3.76 – 3.64 (m, 2H), 2.78, 2.76 (s, s, 3H). LCMS (ESI) calcd. for $C_{15}H_{20}N_5O_5S$ $[M]^+$ 383.1, obsd. 383.0.

Synthesis of 1-^{13}C SAM$_{CA}$

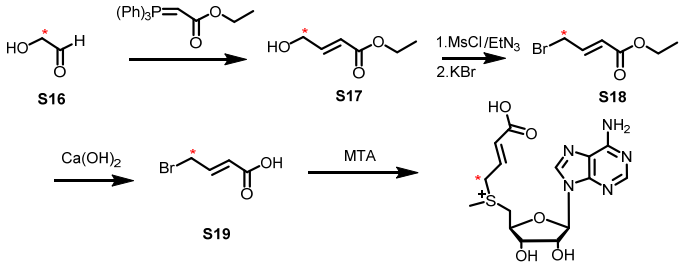

1-^{13}C SAM$_{CA}$ was synthesized according to the same procedure for the synthesis of 2-^{13}C SAM$_{CA}$ by employing [2-^{13}C]glycolaldehyde.

1-^{13}C SAM$_{CA}$ (3:2 mixture of stereoisomers)^{1}H NMR (400 MHz, D_2O) δ 8.37 – 8.29 (m, 2H), 6.70 – 6.53 (m, 1H), 6.05 (d, 1H), 6.02 (dd, J =15.6, 6.8 Hz, 0.4H), 5.88 (dd, J =15.6, 6.8 Hz, 0.6H), 4.76 – 4.71 (m, 1H), 4.65 – 4.52 (m, 2H), 4.48-4.39 (m, 1H), 4.33-4.27 (m, 1H), 3.96-3.90 (m, 1H), 3.84 – 3.71 (m, 2H), 2.83 (m, 3H). LCMS (ESI) calcd. for $C_{15}H_{20}N_5O_5S$ $[M]^+$ 383.1, obsd. 383.0.

Synthesis of 1,1-$^2H_2$ SAM$_{CA}$

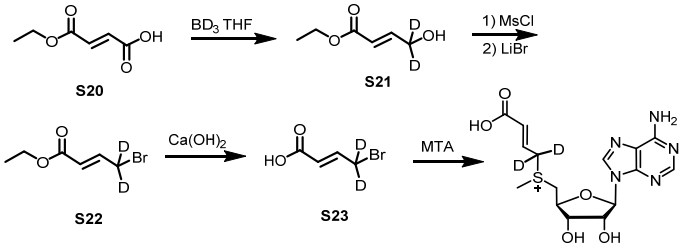

[4,4-$^2H_2$] 4-hydroxyl ethyl crotonate (S21)

Ethyl fumarate (288 mg, 2 mmol) was dissolved in anhydrous THF (1 mL). The solution was cooled to -20℃. Borane-d_3-THF complex solution (1 M, 3 mL, 3 mmol) was added dropwise in 30 min at the same temperature. The resulting mixture was stirred for 30 min at -20℃ and 12 hr at room temperature. The solvent was evaporated under vacuum and the crude product was purified by silica gel column chromatography (hexane:ethyl acetate 5:1) to give **S21** (124 mg, 47% yield). ^{1}H NMR (400 MHz, $CDCl_3$) δ 6.99 (d, J = 15.7 Hz, 1H), 6.06 (d, J = 15.7 Hz, 1H), 4.17 (q, J = 7.1 Hz, 2H), 1.26 (t, J = 7.1 Hz, 3H).

1,1-$^{2}H_2$ SAM_{CA} was synthesized according to the same procedure for the synthesis of 3-^{13}C SAM_{CA} by employing [4,4-$^{2}H_2$] 4-hydroxyl ethyl crotonate, starting from the **S10** preparation step.
1,1-$^{2}H_2$ SAM_{CA} (3:2 mixture of stereoisomers}^{1}H NMR (400 MHz, D_2O) δ 8.24 (d, 2H), 6.54 – 6.37 (m, 1H), 5.98 (d,1H), 5.96 (d, J = 15.6 Hz, 0.4H) 5.81 (d, J = 15.6 Hz, 0.6H), 4.73 – 4.67 (m, 1H), 4.56 – 4.46 (m, 1H), 4.44 – 4.31 (m, 1H), 3.78 – 3.61 (m, 2H), 2.77, 2.75 (s,s, 3H). LCMS (ESI) calcd. for $C_{15}H_{18}D_2N_5O_5S$ $[M]^+$ 384.1, obsd. 384.1.

Synthesis of 1,1,2,3-$^{2}H_4$ SAM_{CA}

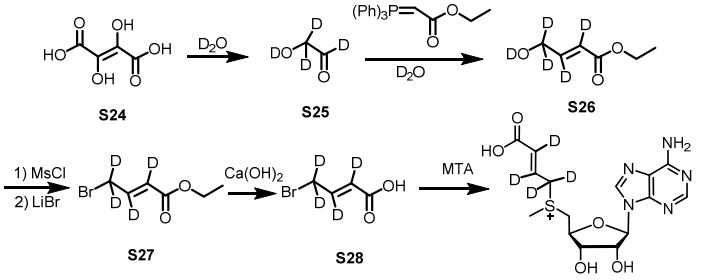

1,1,2,3-$^{2}H_4$ SAM_{CA} was synthesized according to the same procedure for the synthesis of 2-^{13}C SAM_{CA} by employing [1,2,2,3-$^{2}H_4$]glycolaldehyde[5].
1,1,2,3-$^{2}H_4$ SAM_{CA}(3:1 mixture of stereoisomers}^{1}H NMR (600 MHz, D_2O) δ 8.31 (s,s, 2H), 6.03 (s,s, 1H), 4.73-4.67 (m, 1H), 4.58-4.52 (m, 1H), 4.47 – 4.37 (m, 1H), 3.83 – 3.68 (m, 2H), 2.82, 2.81 (s,s, 3H). LCMS (ESI) calcd. for $C_{15}H_{16}D_4N_5O_5S$ $[M]^+$ 386.1, obsd. 386.1.

Q-band EPR and ENDOR
CW ENDOR peaks were strongly influenced by the direction and speed of the rf sweep, a result of slow nuclear spin relaxation system in this intermediate. The observed coupling constants were therefore reported as the average of coupling constants of forward and reverse scan directions. Pulsed ENDOR spectra were collected on a spectrometer described earlier,[2] equipped with a helium immersion dewar for measurements at 2 K. ENDOR measurements employed the Mims pulse sequence (π/2−τ−π/2−T−π/2−τ−echo, RF applied during interval T). For nuclei (N) of spin I = 1/2(^{13}C, ^{1}H) interacting with a S = 1/2 paramagnetic center, the first-order ENDOR spectrum for a single molecular orientation is a doublet with frequencies (ν_+/ν_-),

$$\nu_{\pm} = \nu_{\mathrm{N}} \pm \frac{A}{2} \quad (1)$$

where ν_N is the Larmor frequency and A is the orientation-dependent hyperfine constant. For nuclei with I = 1 (^{2}H), the first-order ENDOR condition can be written:

$$\nu_{\pm}(\pm) = \left|\nu_{\mathrm{N}} \pm \frac{A}{2} \pm \frac{3P}{2}\right| \quad (2)$$

where P is the orientation-dependent quadrupolar splitting. But this splitting was unresolved in this study because it was buried in broader ENDOR line-width. For a nucleus with hyperfine coupling, A, Mims pulsed ENDOR has a response R that depends on the product, $A\tau$, according to the equation.

$$\mathrm{R} \sim [1 - \cos(2\pi A\tau)] \quad (3)$$

This function has zeros, corresponding to minima in the ENDOR response (hyperfine "suppression holes"), at $A\tau$ = n; n = 0, 1, ..., and maxima at $A\tau$ = (2n + 1)/2; n = 0, 1, ...[6] The "holes" at A = n/τ, n = 1, 2, 3, ..., can be adjusted by varying τ. However, the "central", n = 0, hole at $\nu = \nu_N$ persists regardless. This can be of significance in distinguishing a tensor that is dominated by anisotropic interactions from one that is dominated by isotropic ones. The latter would never lead to ENDOR intensity near ν_N; the former does so for certain orientations, but the ν = 0 Mims hole tends to diminish the differences between the two cases.

Badan derivative reaction

A portion of enzymatic reaction of PhDph2 with SAM_{CA} for ^{1}H-NMR was treated with KF and 6-bromoacetyl-2-dimethylaminonaphthalene (badan) following the reported procedure[7]. The reaction was extracted by dichloromethane. The organic layer was evaporated and redissolved in acetonitrile before analysis by LC-MS.

Cryoreduction

To confirm the oxidation state of the cluster in CA, we applied cryoreduction/annealing techniques to CA. Figure S24 shows EPR spectra for CA before (blue) and after (red) cryoreduction/annealing. The sample was exposed to γ-irradiation in the quartz EPR tube at 77 K and annealed at 240 K for 1 min to remove the majority of signals from free radicals. Although the resulting EPR spectrum after annealing still shows a strong signal around g~2 from the radicals in the quartz tube, the spectrum clearly shows that the intensity of the g_1 feature of CA is not decreased, as would be expected if it was associated with a $[4Fe\text{-}4S]^{3+}$ cluster. In contrast at $g < 2$ there appears the signal from $[4Fe\text{-}4S]^{1+}$ cluster that is formed by cryoreduction of the $[4Fe\text{-}4S]^{2+}$ cluster that remained after turnover. This observation of cryoreduction of $[4Fe\text{-}4S]^{2+}$ but not of CA supports the inference that the CA signal is associated with a $[4Fe\text{-}4S]^{1+}$ cluster, not a $[4Fe\text{-}4S]^{3+}$ cluster.

Comments about the Mössbauer spectra.

The 4.2-K/53-mT Mössbauer spectrum of as-isolated *Ph*Dph2 (Figure S26A) is dominated by a quadrupole doublet with parameters typical of $[4Fe\text{-}4S]^{2+}$ clusters (isomer shift of $\delta = 0.45$ mm/s and quadrupole splitting parameter of $\Delta E_Q = 1.15$ mm/s) and identical to those reported previously for *Ph*Dph2.[4] This doublet accounts for ~95% of the total intensity of the spectrum. Together with the stoichiometry of 1.4 Fe per *Ph*Dph2, this result suggests the presence of 0.35 [4Fe-4S] clusters per *Ph*Dph2. Consistent with these results, an identical EPR sample does not reveal the presence of Fe/S clusters with an $S = 1/2$ ground state ($[2Fe\text{-}2S]^+$, $[4Fe\text{-}4S]^+$, $[4Fe\text{-}4S]^{3+}$, or $[3Fe\text{-}4S]^+$). The Mössbauer parameters are slightly different at 120 K ($\delta = 0.43$ mm/s, $\Delta E_Q = 1.02$ mm/s). Addition of the SAM_{CA} substrate analog perturbs the Mössbauer spectrum slightly (Figure S26B); the apparent quadrupole splitting is decreased by ~0.1 mm/s at 120 K (0.91 mm/s). When the *Ph*Dph2 and SAM_{CA} mixture is treated with excess dithionite for 9 minutes at room temperature, the 4.2-K/53-mT spectrum changes noticeably (Figure S26C). Analysis of the spectrum reveals three major components in the sample: (i) the CA product, which exhibits a magnetically split subspectrum due to its half-integer electron spin ground state (~55% of total intensity); (ii) the *Ph*Dph2 and SAM_{CA} mixture (~35% of total intensity); and (iii) a small amount (~10%) of one (or more) complexes of unknown identity. Consistent with this result, an identical EPR sample reveals the formation of 150 μM (55% of 270 μM [4Fe-4S]-loaded *Ph*Dph2) of the CA product complex, which has an $S = 1/2$ ground state (see Figure 1 of main manuscript). As expected for a complex with $S = 1/2$ ground state, the spectrum of the sample strongly depends on the orientation of the external field relative to that of the γ-beam (Figure S27). Moreover, the magnitude of the magnetic splitting is comparable to the splittings observed for the $[4Fe\text{-}4S]^+$ cluster of *Bacillus stearothermophilus* ferredoxin (Figure S27, green lines) and for the $[4Fe\text{-}4S]^{3+}$ cluster of *Allochromatium vinosum* high-potential iron-protein (HIPIP) (Figure S27, red lines). Because the simulation of the CA complex is dependent on a large number of spin Hamiltonian parameters, which are strongly correlated, it is difficult to determine them unambiguously. Moreover, the features associated with $[4Fe\text{-}4S]^+$ and $[4Fe\text{-}4S]^{3+}$ clusters are similar, making the distinction of these cluster types difficult.

In order to simplify the complexity of the spectra, we recorded 120-K/zero-field spectra, because under these experimental conditions, the relaxation of the electronic spin is fast and therefore the CA complex gives rise to quadrupole doublets. Comparison of the 120-K/zero-field spectra recorded prior to dithionite-reduction (Figure S28B) and after dithionite reduction (Figure S28C) reveals that the high-energy line at ~1mm/s is shifted to higher energies, suggesting that dithionite reduction results in an *increase* of the average isomer shift. These differences are caused by the generation of ~55% CA cluster and ~10% of the unknown product from the *Ph*Dph2 and SAM_{CA} mixture. If we assume that the [4Fe-4S] cluster of the CA product state contains one valence-delocalized Fe_2-pair (the spectral features of which is expected not to change significantly upon reduction), the observed differences are caused primarily by the spectral features of the Fe_2-pair of CA, which includes the unique Fe site coordinated by the α-sulfinyl-3-butenoic acid product (~28% of total Fe, half of the Fe associated with the CA complex), and the unknown product (~10% of total Fe). Analysis of the spectra suggests that the average isomer shift of the two Fe sites of the unique pair of the CA product cluster increases by ~0.15 mm/s (see Table S2). While the increase of the average isomer shift upon treatment with dithionite is unequivocal, the interpretation is not straightforward. First, the increased isomer shift could be taken as evidence that the cluster is best described as a $[4Fe\text{-}4S]^{+}$-cluster having a diferrous pair and a mixed-valent pair (i.e. resonance structure **a** in Figure 3 of the main manuscript). Second, the increased isomer shift could also be due to the coordination of theα-sulfinyl-3-butenoic acid product to one of the Fe sites of the cluster. Indeed, binding of substrates or analogs to the unique Fe site of Cys_3-coordinated [4Fe-4S] clusters of radical SAM enzymes[8] and aconitase[9] is known to increase the isomer shift of the unique Fe site considerably without a change of the formal oxidation state. Therefore, the modestly increased isomer shift could also be rationalized by resonance structure **b** in Figure 3 of the main manuscript, for which the decreased isomer shift of the diferric pair of the formally $[4Fe\text{-}4S]^{3+}$ cluster could be compensated by the larger increase of the isomer shift due to binding of the α-sulfinyl crotonate product. Thus, while the available Mössbauer data indicates that the average isomer shift increases modestly in the CA product complex, this observation does not allow us to unequivocally determine the real, physical oxidation state of the cluster.

Generation of the EPR signal of CA with the reaction product.

A reaction (250 μM PhDph2, 50 mM dithionite, and 10 mM SAM_{CA} in 105ul of 100 mM phosphate buffer with 150 mM sodium chloride, pH 7.4) was set up in an anaerobic chamber. The reaction was incubated for 2 hr at room temperature to complete. The mixture was transferred to a Millipore Microcon YM-10 filter unit and centrifuged at 14000g for 10 min × 3. Another 100ul buffer was added to the filter to elute most of product. A portion of the filtrate (25ul out of 100ul) was added to a fresh aliquot of enzyme solution (480 μM PhDph2, 20 mM dithionite in 25ul). The mixture was incubated for 5 min at room temperature and transferred to EPR tube before frozen in liquid N_2. The tube was sealed in the anaerobic chamber and taken out for EPR analysis.

For the α-sulfinyl-3-butenoic acid decomposition experiment. The steps are all the same as above. The only difference is after filtration of the protein, the product mixture was incubated at 30℃ for 12 hr to let α-sulfinyl-3-butenoic acid decompose (Confirmed by ^{1}H-NMR as shown in Figure S21).

B. Supplementary Figures

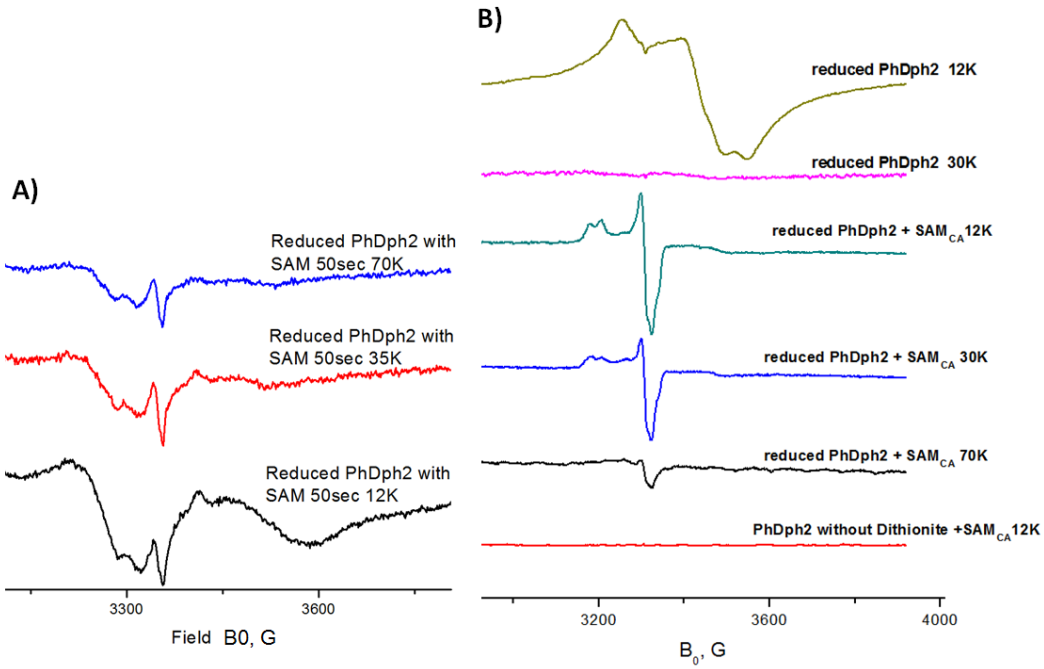

Figure S1. Variable-temperature EPR spectra of a hand-quench experiment, in which PhDph2 was incubated with SAM (**A**) and SAM_{CA} (**B**) and treated with sodium dithionite. The small radical signals ($g \sim 2$) in each spectra of **A** would be from extra amount of dithionite and the broad signal at around 3300 G would be from cavity background.

.

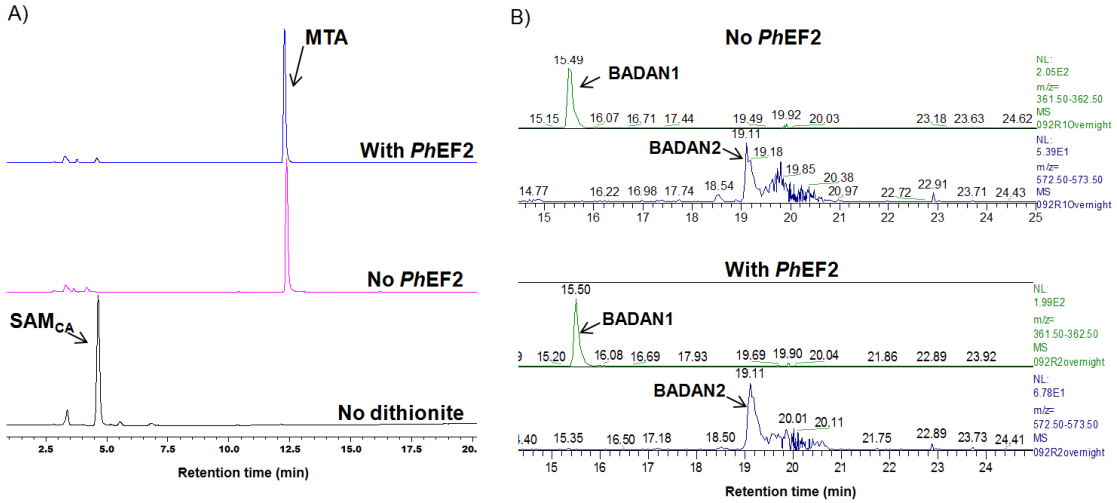

Figure S2: PhDph2 and SAM_{CA} reaction has the same reaction products with and without substrate protein PhEF2. A) HPLC analysis of reaction product. B) Detection of Badan derivatives of the reaction products by LC–MS. The mass spectroscopy (MS) traces (ion counts for specific compounds) are shown for the reaction without PhEF2 (top) and with PhEF2 (bottom).

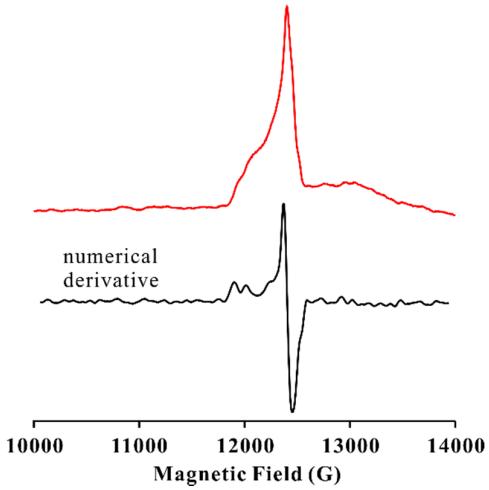

Figure S3. 35 GHz CW EPR spectrum and numerical derivative spectrum for PhDph2 with SAMca. *Experimental conditions*: microwave frequency = 34.99 GHz, microwave power = 1 mW, 100 kHz modulation amplitude = 0.7 G (top) Rapid-passage absorption mode spectrum (bottom) numerical derivative spectrum. The splitting at g_1 is approximately 100 G.

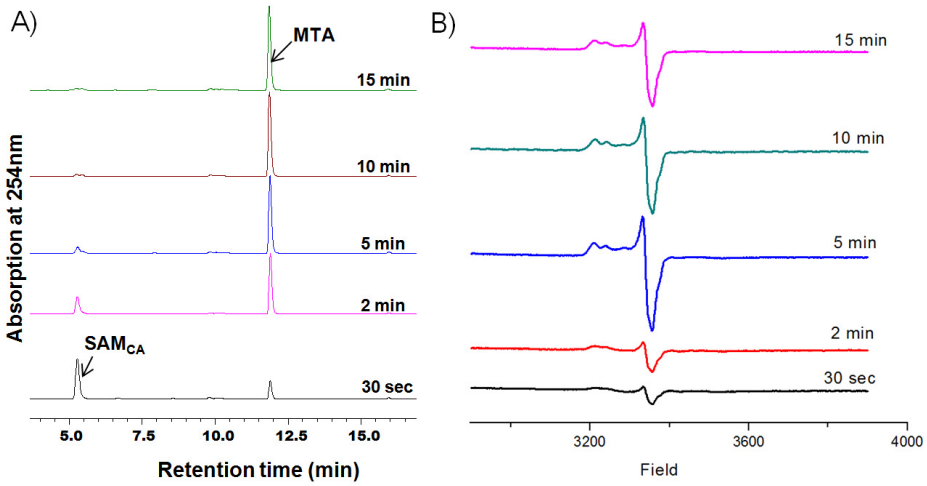

Figure S4. A) HPLC trace of time-dependent formation of product MTA. B)Time-dependent formation of the X-band EPR signal of complex CA at 30K.

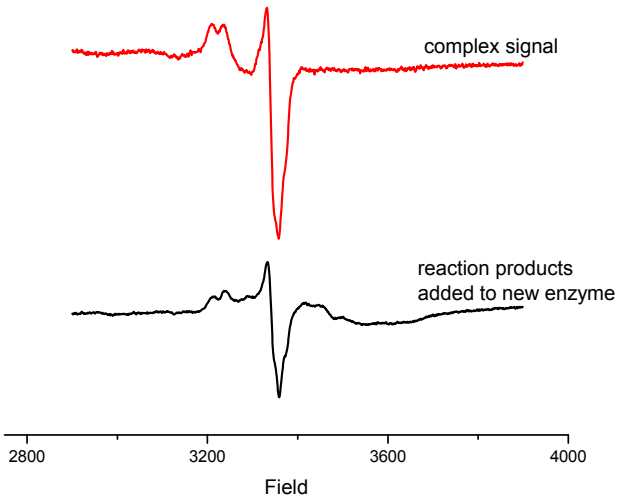

Figure S5. X-band EPR showing the regeneration of the complex signal by mixing the products with new aliquots of enzyme

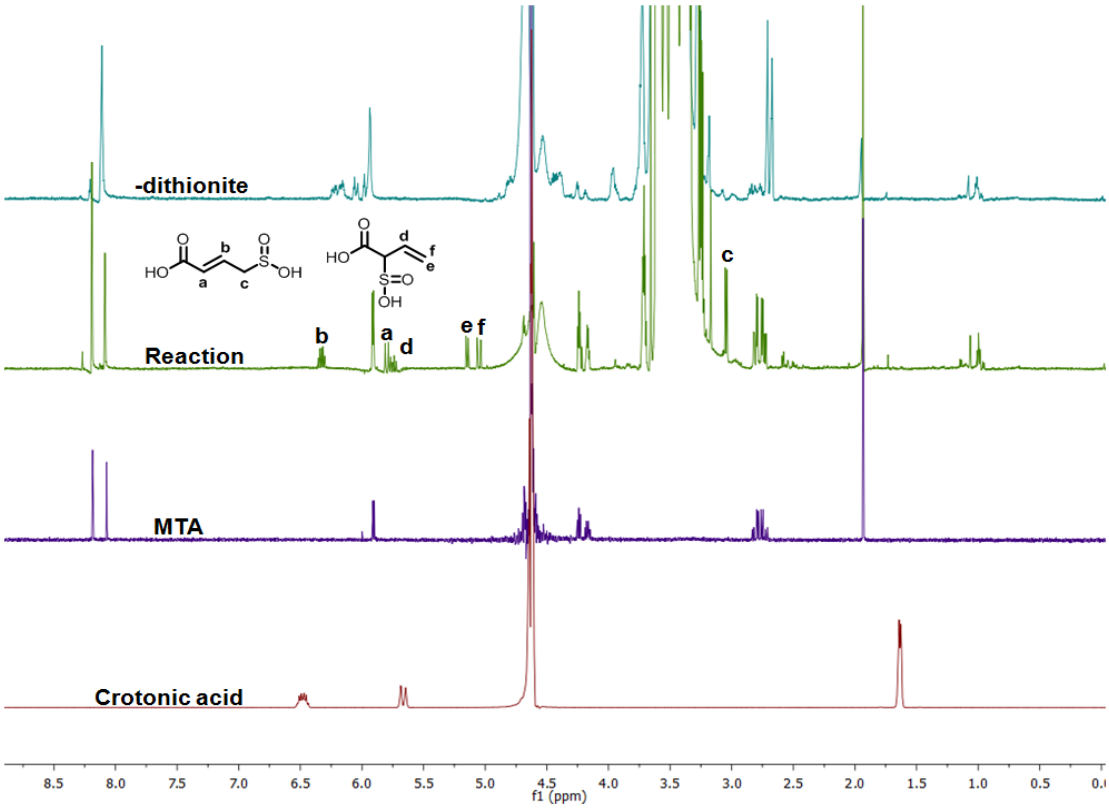

Figure S6. Reaction products of SAM_{CA} with *Ph*Dph2 detected by ^{1}H-NMR. Peaks a, b and c are from γ-sulfinylcrotonic acid. Peaks d, e and f are from the isomer α-sulfinyl-3-butenoic acid. No signals from crotonic acid were detected in the reaction.

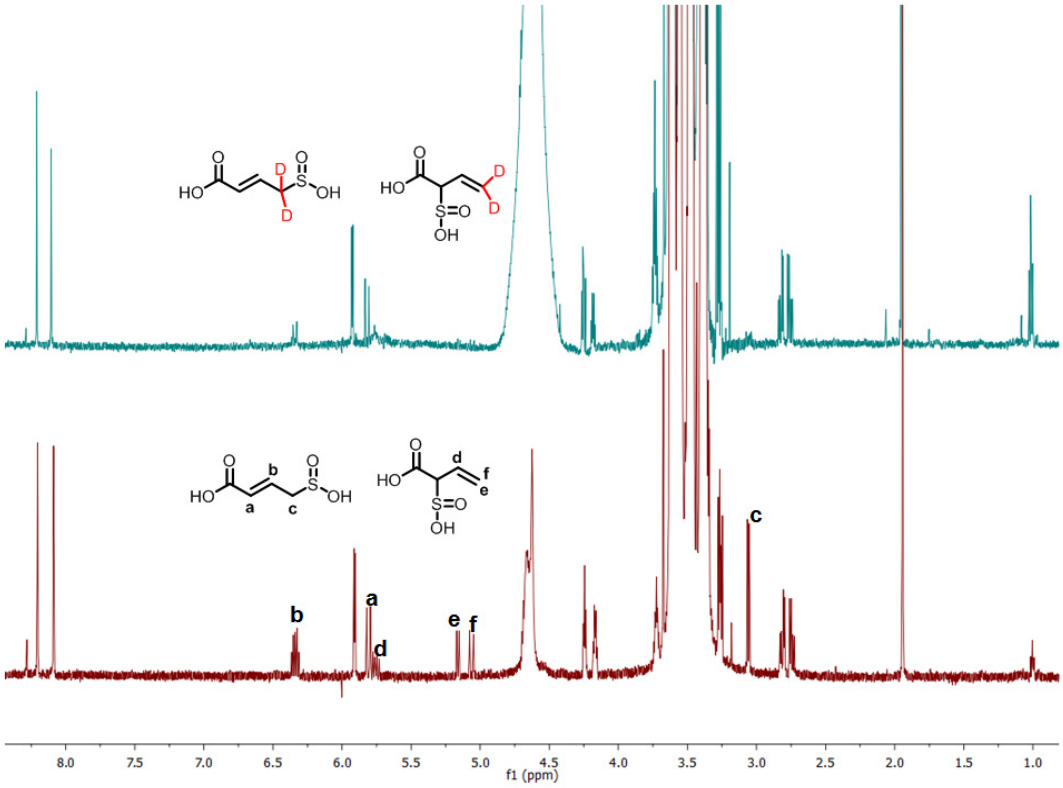

Figure S7. ^{1}H NMR spectra of SAM_{CA} and 1,1-$^{2}H_2$ SAM_{CA} with *Ph*Dph2

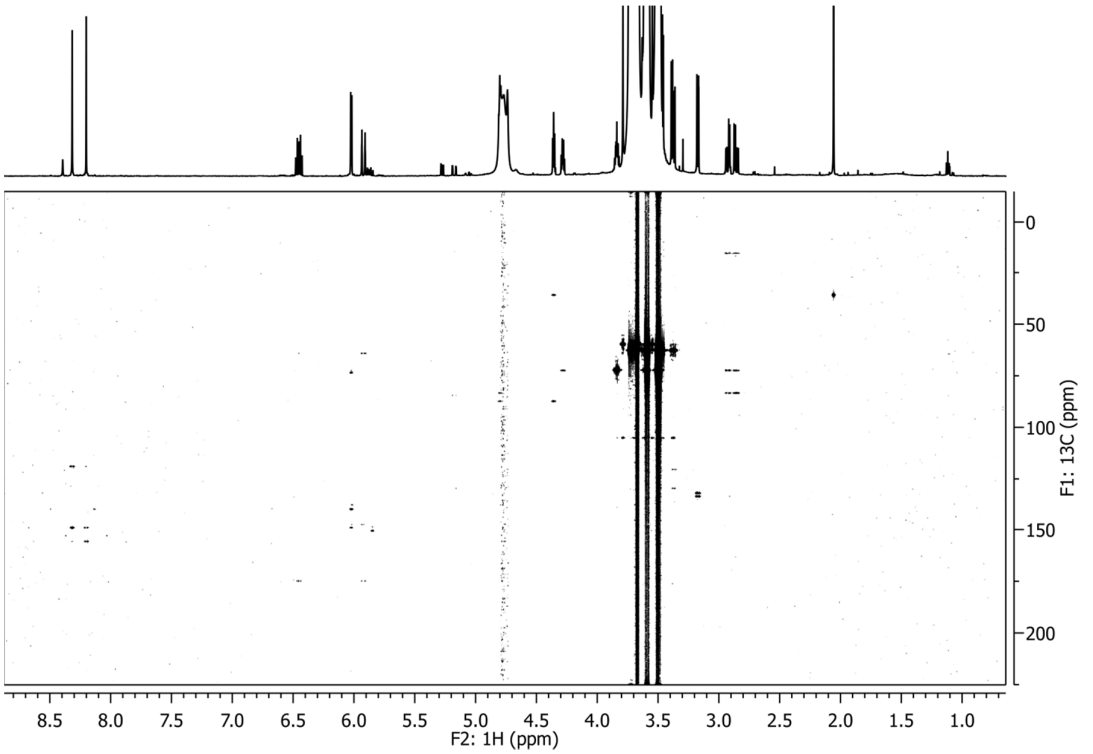

Figure S8. $^{1}H/^{13}C$ HMBC NMR spectrum of *Ph*Dph2 with SAM$_{CA}$.

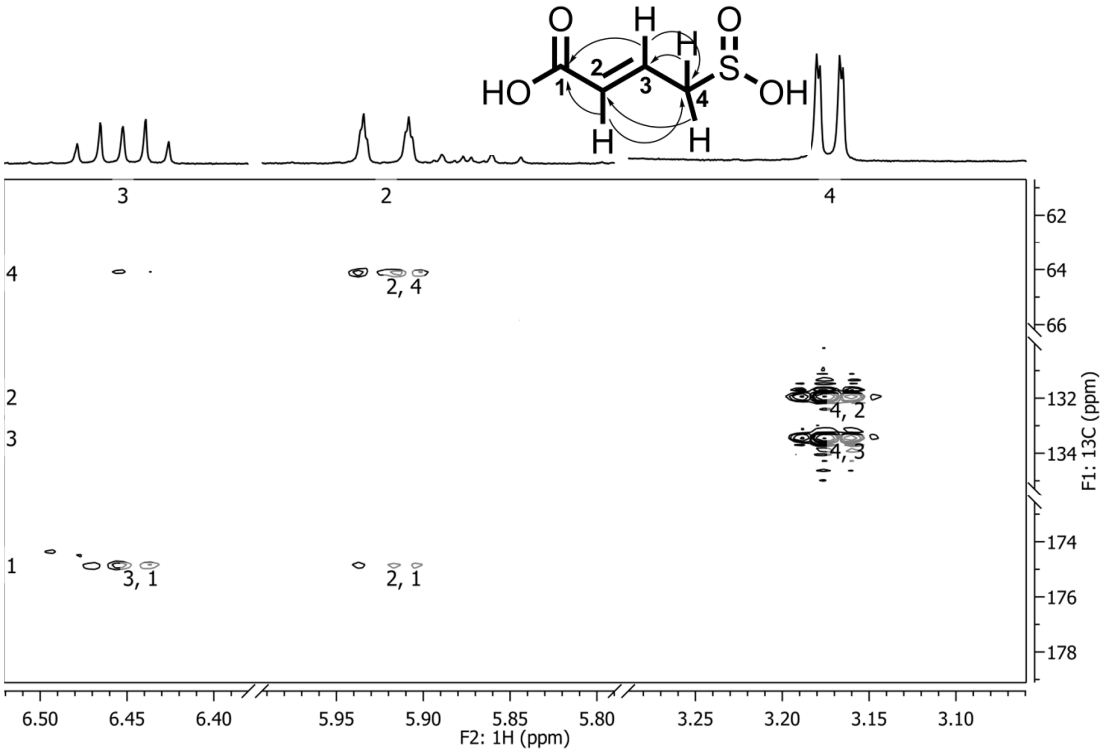

Figure S9. Enlarged $^{1}H/^{13}C$ HMBC NMR spectrum of *Ph*Dph2 with SAM$_{CA}$ to display areas of interest. The correlations are marked. The generation of γ-sulfinyl crotonic acid is confirmed by the cross peaks. The other isomer, α-sulfinyl-3-butenoic acid, is not stable. The instability of this compound is likely due to the acidity of the α-proton due to two adjacent strong electron-withdrawing groups, and potential nucleophilic addition to the isomerized alkene.[10]. Signals from it disappeared while the HMBC spectrum was collected.

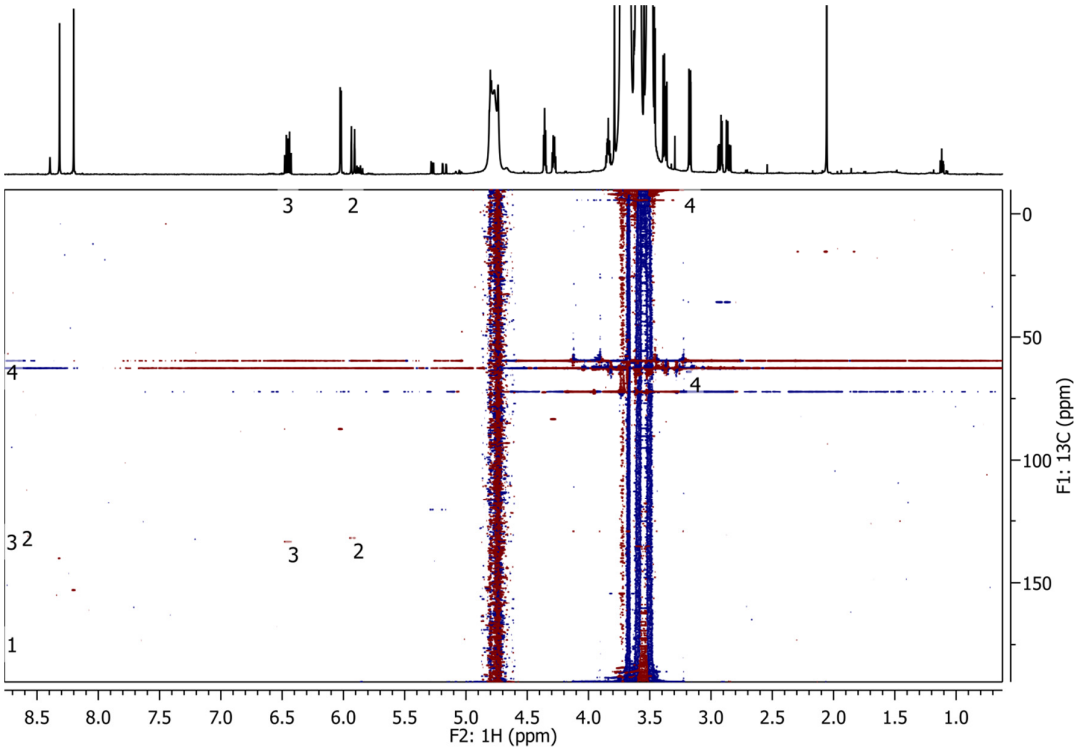

Figure S10. $^{1}H/^{13}C$ multiplicity-edited HSQC spectrum of *Ph*Dph2 with SAM_{CA}. Red and blue contours correspond to CH/CH3 and CH2 correlations, respectively. The numbers indicate assignments in γ-sulfinyl crotonic acid.

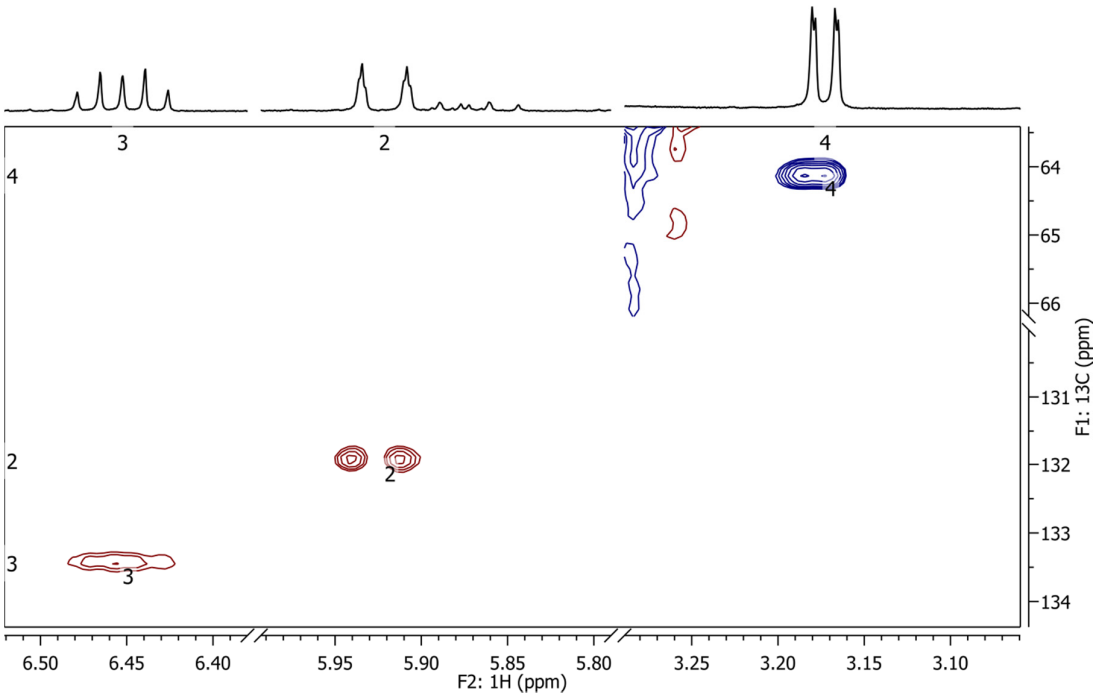

Figure S11. Enlarged $^{1}H/^{13}C$ multiplicity-edited HSQC spectrum of *Ph*Dph2 with SAM_{CA} showing areas of interest. Red and blue contours correspond to CH/CH3 and CH2 correlations, respectively. The assignments are indicated by the numbers.

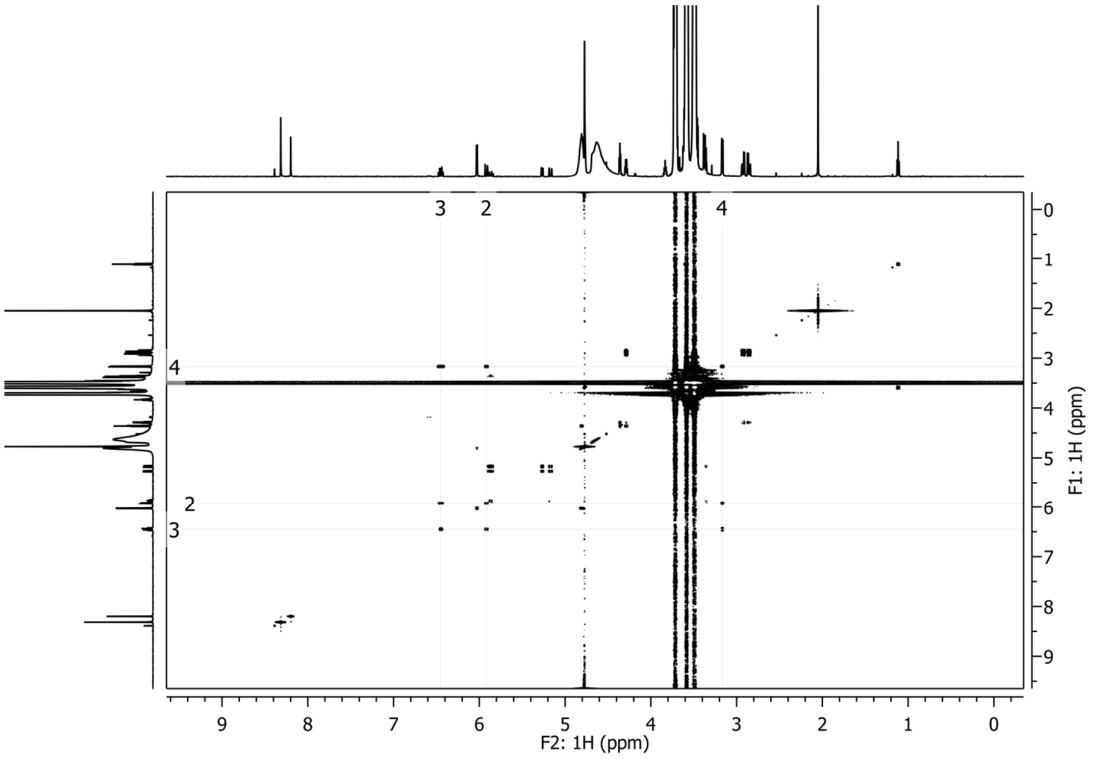

Figure S12. Magnitude-mode gradient COSY spectrum of *Ph*Dph2 with SAM_{CA}. Numbers indicate assignments in γ-sulfinyl crotonic acid.

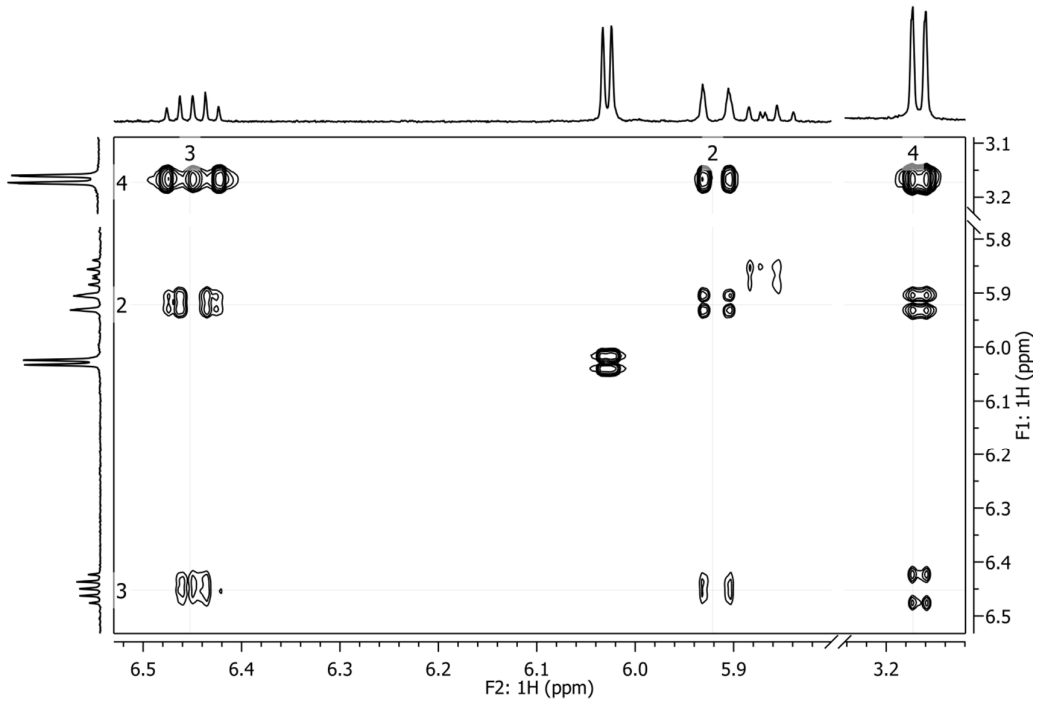

Figure S13. Enlarged magnitude-mode gradient COSY spectrum of *Ph*Dph2 with SAM_{CA} showing areas of interest.

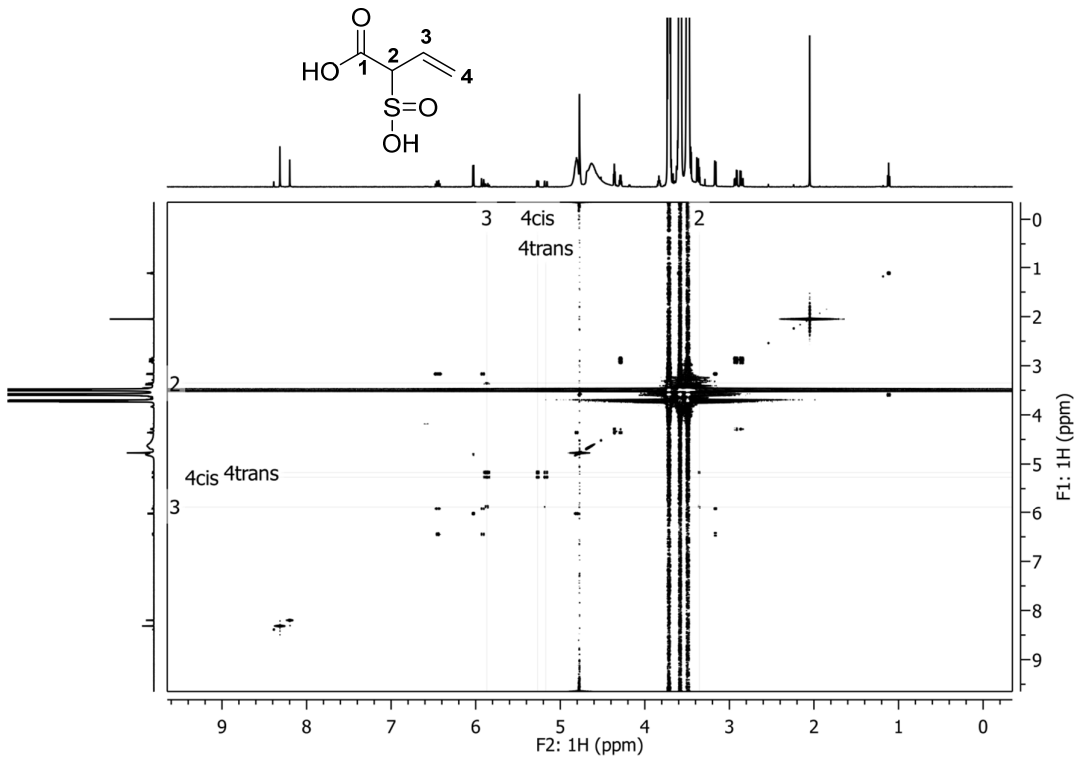

Figure S14. Magnitude-mode gradient COSY spectrum of *Ph*Dph2 with SAM_{CA}. Numbers indicate assignments in α-sulfinyl crotonic acid.

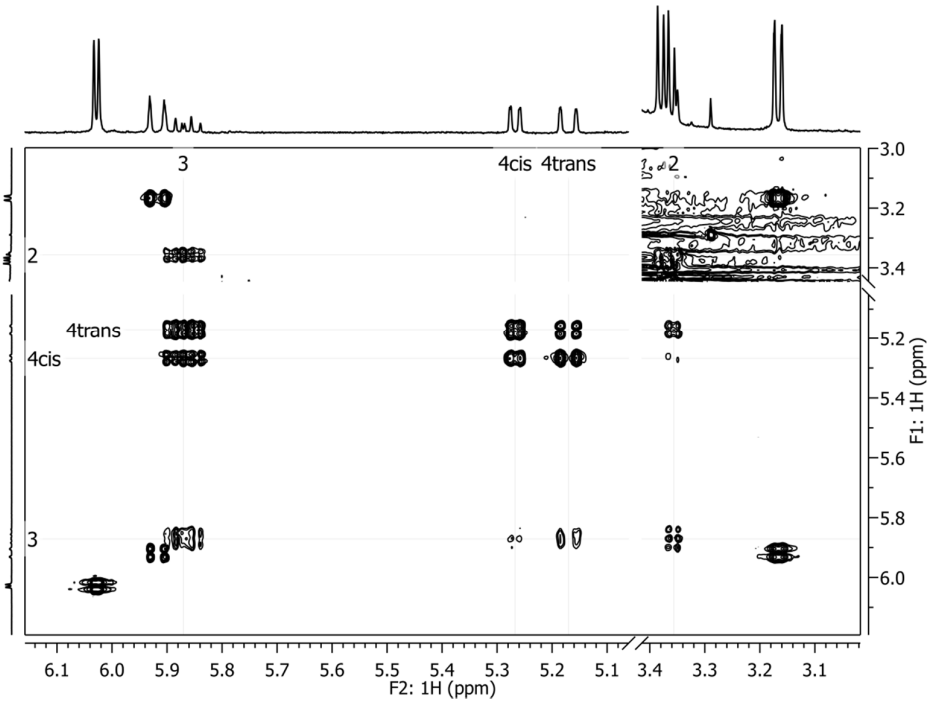

Figure S15. Enlarged magnitude-mode gradient COSY spectrum of *Ph*Dph2 with SAM_{CA} showing areas of interest. Numbers indicate assignments in α-sulfinyl crotonic acid.

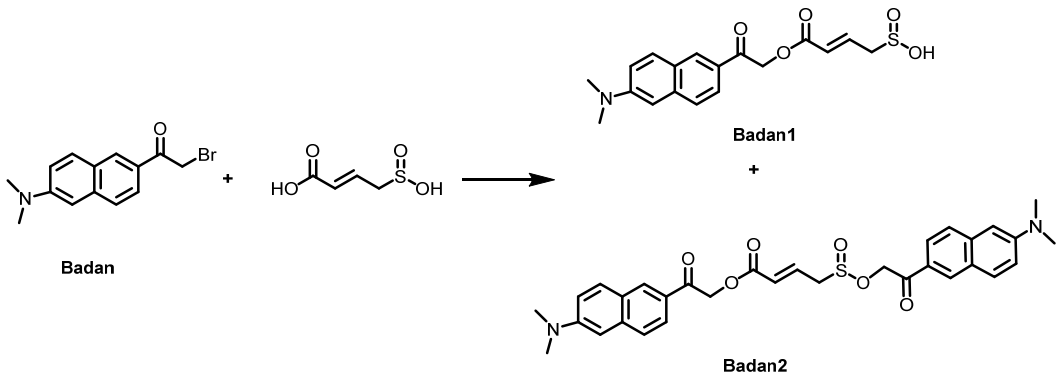

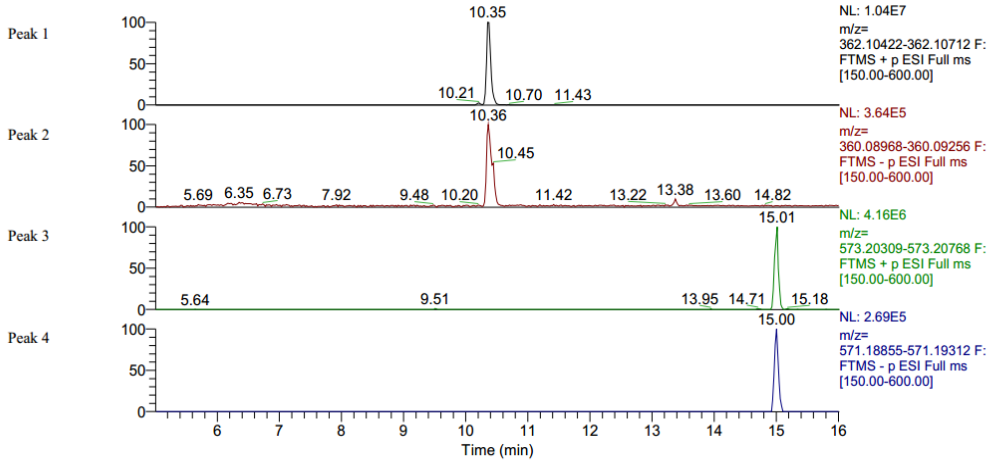

#	Comp. Index	Compound Name	Formula	Detected m/z	Delta (ppm)	Expected RT	Actual RT	Intensity	Adducts			Fragments		
									H+	NH4+	Na+	1	2	3
1	1	bandan1	C18H19N1O5S	362.10535	-0.9	0.00	10.35	10381131	Y*	-	-	-	-	-
2	2	bandan1	C18H19N1O5S	360.09134	0.6	0.00	10.36	362042	Y*	-	-	-	-	-
3	3	bandan2	C32H32N2O6S	573.20508	-0.5	0.00	15.01	4156190	Y*	-	-	-	-	-
4	4	bandan2	C32H32N2O6S	571.19214	2.3	0.00	15.00	268899	Y*	-	-	-	-	-

Figure S16. The badan derivatization reaction and high resolution mass spectra for the products. (only show γ-sulfinylcrotonic acid, α-sulfinyl-3-butenoic acid gives the same reaction and mass)

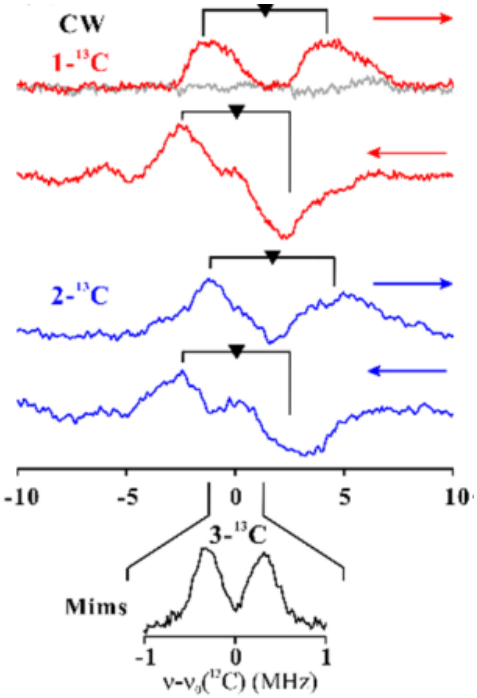

Figure S17. 35 GHz CW ^{13}C ENDOR spectra for the PhDph2 complex CA with 1,2-^{13}C-labeled SAM_{CA} collected at g_2 . The directions of the CW rf sweep are as indicated. **Inset:** Mims ENDOR spectra of 3-^{13}C SAM_{CA}. (Unfavorable relaxation rates and low signal intensities precluded the characterization of 1, 2-^{13}C labeled SAM_{CA} by 35 GHz Davies pulsed and stochastic CW ENDOR methods.) *Experimental conditions*: CW; MW frequencies = 34.8 ~ 34.9 GHz, field modulation frequency/amplitude = 100 kHz/0.7 G, rf sweep rate = 1 MHz/s, T = 2 K, Mims; MW frequency = 34.8 GHz, MW pulse length ($\pi/2$) = 50 ns, τ = 500 ns and T = 2 K.

Note：Slow nuclear relaxation causes the CW spectra to 'shift' in the direction of the rf sweep, and to differ in appearance between 'positive' and 'negative' sweep directions, a common difficulty with this technique. However, comparison of the spectra collected with the two sweep directions allows the spectra to be centered at the ^{13}C Larmor frequency and the hyperfine couplings to be reliably measured.

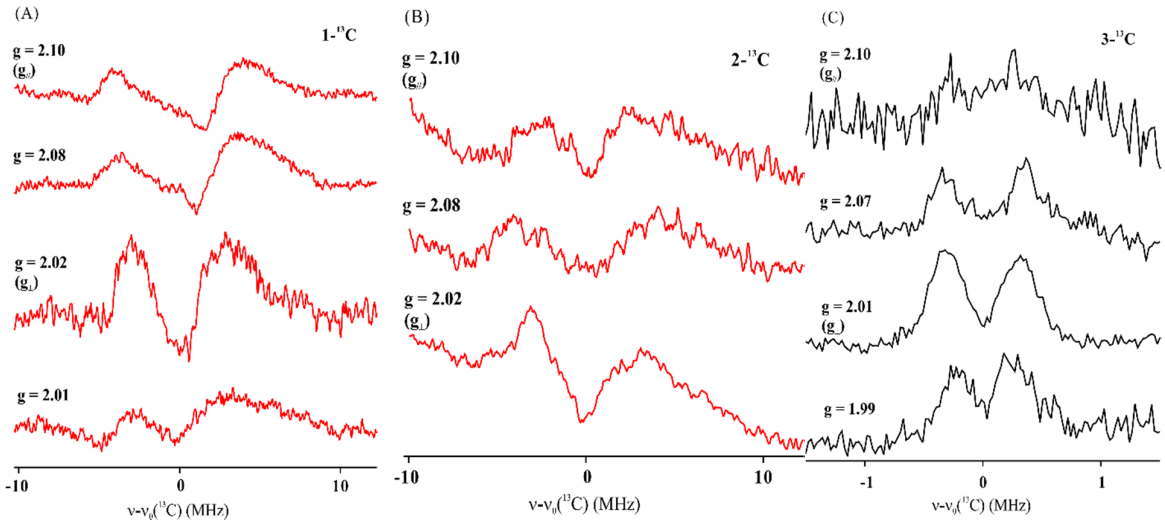

Figure S18. 2D field-frequency pattern ^{13}C ENDOR for complex CA with ^{13}C labeled SAM$_{CA}$. (A) and (B) are CW ENDOR and (C) is Mims ENDOR. Experimental conditions are same as **Figure S17**.

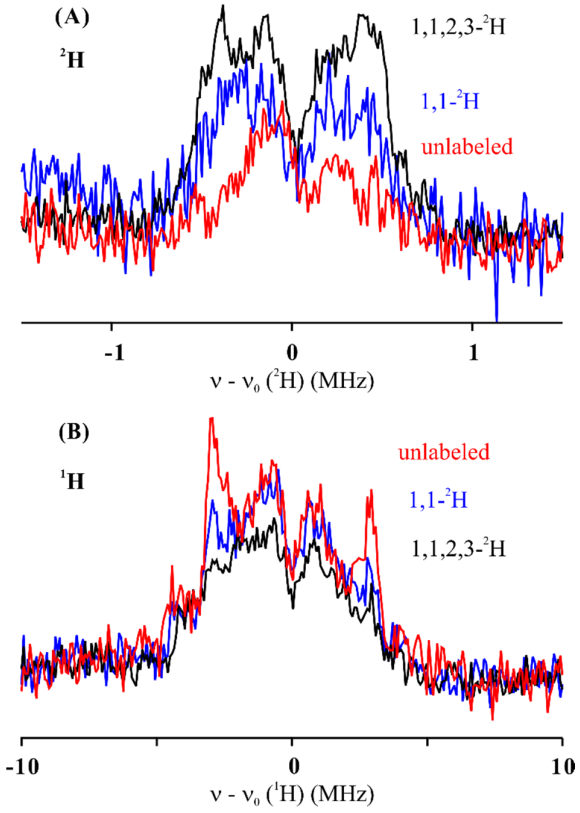

Figure S19. (A) ^{2}H Mims and (B) ^{1}H Davis ENDOR for PhDph2 complex CA with ^{1,2}H-labeled SAM$_{CA}$. Experimental conditions for Mims ENDOR are same as **Figure S17**. *Experimental conditions*: Davies; MW frequency = 34.8 ~ 34.9 GHz, MW pulse length, (π) = 120 ns, τ = 600 ns and T = 2 K.

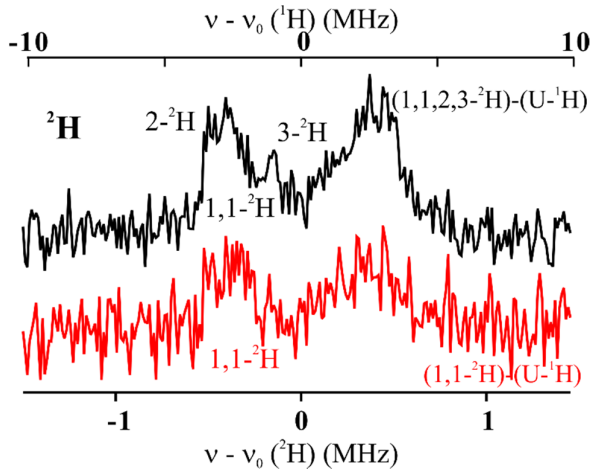

Figure S20. ^{2}H Mims ENDOR difference spectra for PhDph2 complex CA generated by subtracting spectra for natural abundance SAM$_{CA}$ from those for ^{2}H-labeled, as indicated. Spectra were collected at g_2 and normalized by EPR echo height. *Experimental conditions*: MF = 34.8 ~ 34.9 GHz, MW pulse length, (π/2) = 50 ns, τ = 500 ns and T = 2 K.

Note： **Figure S20** displays ^{2}H Mims ENDOR spectra as obtained by subtracting the normalized spectrum for unlabeled SAM$_{CA}$, which exhibits features around the ^{2}H Larmor frequency attributable to ^{14}N double quantum transitions, from the corresponding spectra of the complex with the deuterated SAMca (**Figure S19**). The resulting Mims ^{2}H difference spectrum of 1,1-^{2}H SAM$_{CA}$ (**Figure S20**) exhibits a doublet of broad peaks split by A(^{2}H) ~ 0.8 MHz, corresponding to A(1,1-^{1}H) ~ 5 MHz, and broadened by the ^{2}H (I = 1) quadrupole interaction; the corresponding Davies ^{1}H difference spectra show the same doublet (**Figure 2B**), which appears sharper in part because the I = ½ ^{1}H has no quadrupole interaction. The Mims difference spectrum of 1,1,2,3-^{2}H SAM$_{CA}$ shows a similar pattern, but with greater intensity and perhaps with enhanced intensity near the Larmor (zero) frequency in the spectra, which is tentatively assigned to a ^{2}H signal with a smaller coupling; the Davies difference again shows greater intensity of the A(^{2}H) ~ 0.8 MHz doublet. In the context of the ^{13}C couplings, we interpret these observations to mean that 2-^{2}H contributes to the signal and has a similar hyperfine coupling constant as the 1,1-^{2}H doublet (A(^{2}H) ~0.8 MHz). The putative response with smaller coupling is assigned to 3-^{2}H, with A(3-^{2}H) ~ 0.2 MHz, corresponding to A(3-^{1}H) ~ 1.3 MHz.

Table S1. Hyperfine Tensors (MHz) of ^{13}C ENDOR

	A_1, A_2, A_3 (MHz)	A_{iso} (MHz)	T_1, T_2, T_3 (MHz)
1-^{13}C	8, 6, 6	6.7	1.3, -0.7, -0.7
2-^{13}C	5, 7.5, 7.5	6.7	1.7, -0.8, -0.8
3-^{13}C	0.7, 0.75, 0.25	0.57	-0.13, -0.18, 0.32

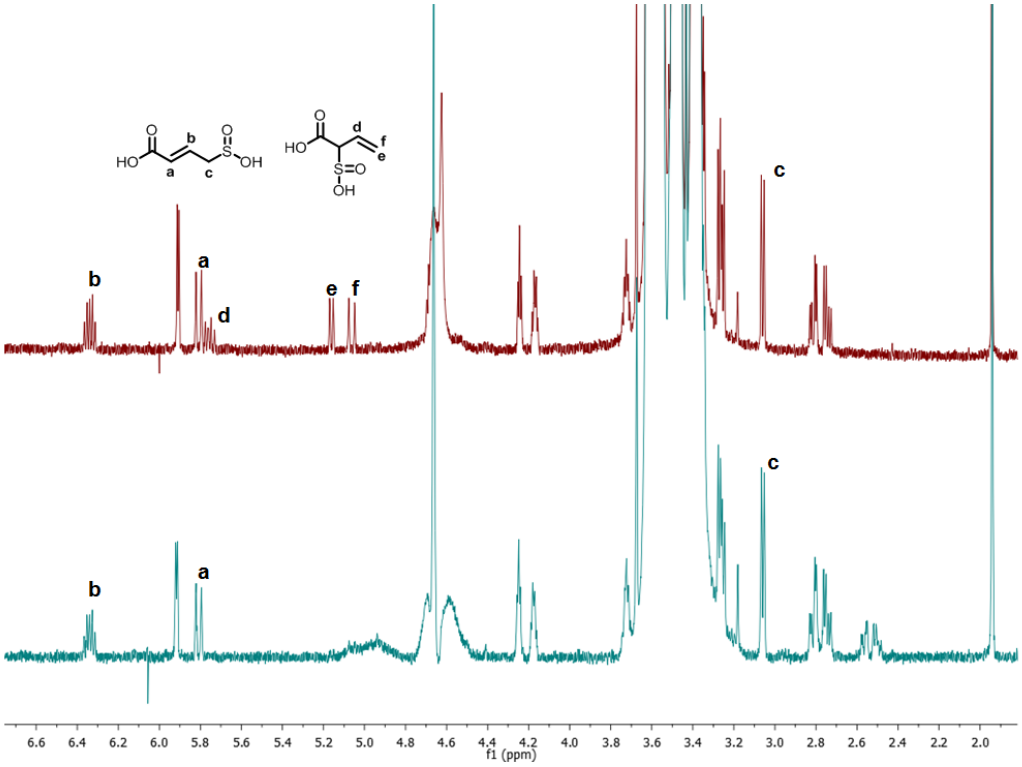

Figure S21. ^{1}H NMR spectra of the reaction products showing the decomposition of α-sulfinyl-3-butenoic acid. Upper spectrum: detected right after the reaction. Lower spectrum: detected after incubation for 12 hr at 30℃.

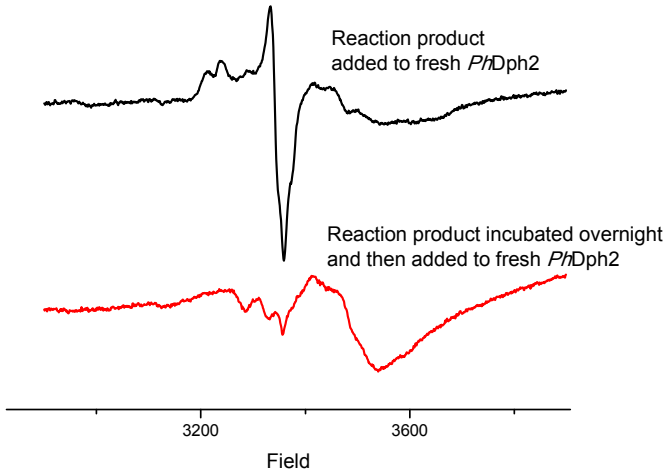

Figure. S22. X-band EPR showing that the mixture containing only the γ-sulfinylcrotonic acid product failed to regenerate the complex signal with new aliquots of enzyme after α-sulfinyl-3-butenoic acid decomposed.

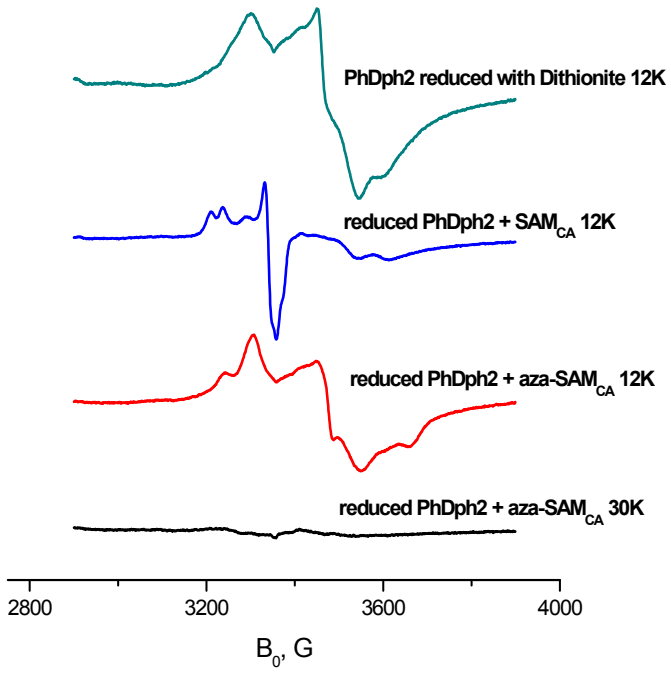

Figure S23. X-band EPR Spectra of PhDph2 with SAM$_{CA}$ and aza-SAM$_{CA}$.

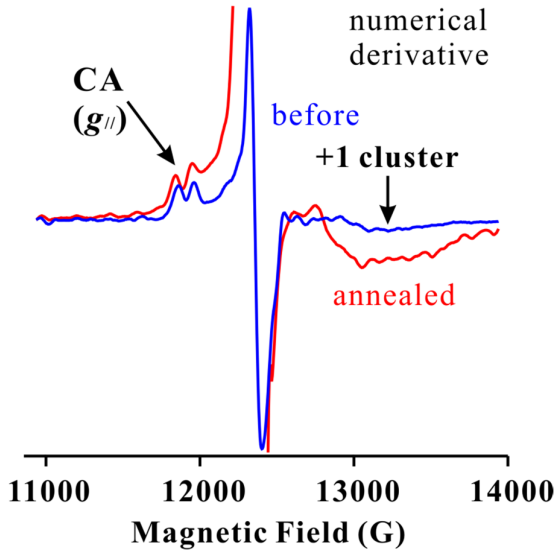

Figure S24. 35 GHz CW EPR spectra for CA, cryoreduced CA and after annealing at 240 K for 1 min. *Experimental conditions*: microwave frequency = 34.99 GHz, microwave power = 1 mW, 100 kHz modulation amplitude = 0.7 G and T = 2 K.

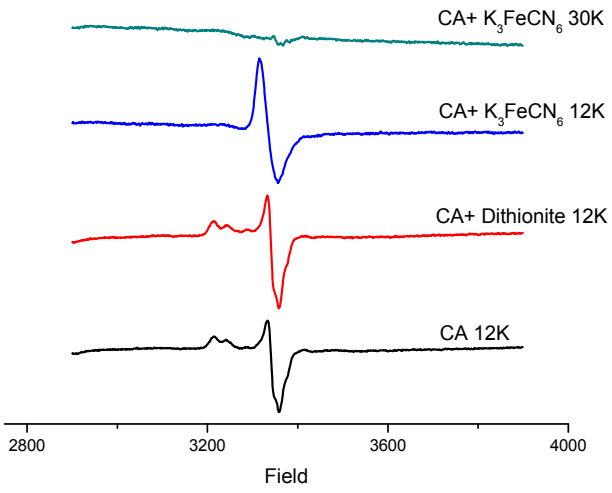

Figure S25. X-band EPR spectra of the redox experiments with CA (Chemically reduced by extra dithionite or oxidized by K_3FeCN_6).

Table S2: Mössbauer parameters obtained from analysis of the 120-K/zero-field spectra.

State	δ(mm/s)/ ΔE_Q(mm/s)	(%)	δ(mm/s)/ ΔE_Q(mm/s)	(%)	δ(mm/s)/ ΔE_Q(mm/s)	(%)	δ(mm/s)/ ΔE_Q(mm/s)	(%)
As-purified *Ph*Dph2	0.43 1.01	94			-	-	0.80 1.65	6
As-purified *Ph*Dph2 +SAM_{CA}	0.41 0.91	87			-	-	0.8 1.65	6
***Ph*Dph2 +SAM_{CA} + dithionite**	0.47 1.04	63	0.61 1.14	26	1.2 2.95	5	0.87 1.80	6

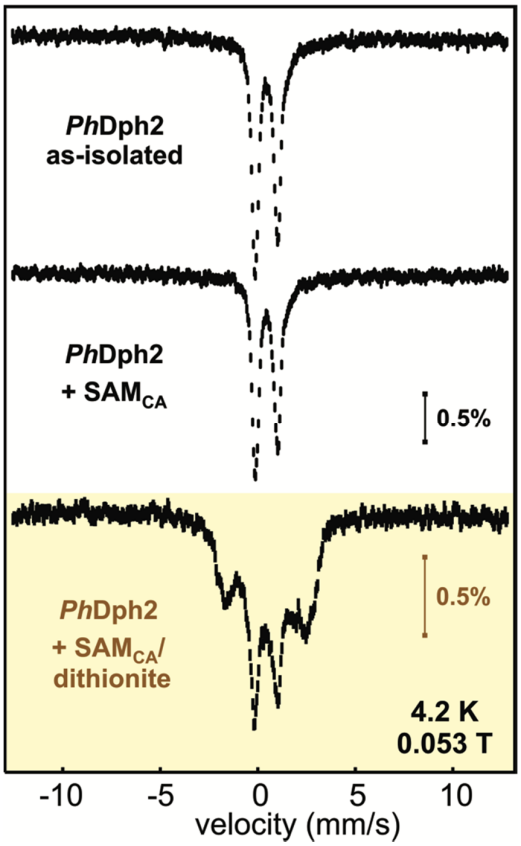

Figure S26: 4.2-K/53-mT Mössbauer spectra of anaerobically isolated (AI) *Ph*Dph2 (top), AI *Ph*Dph2 incubated with SAM_{CA} in the absence of a reducing agent (middle), and of the CA complex formed by incubation of AI *Ph*Dph2 with SAM_{CA} followed by treatment with excess dithionite for 9 minutes (bottom). The magnetic field was applied parallel to the γ beam.

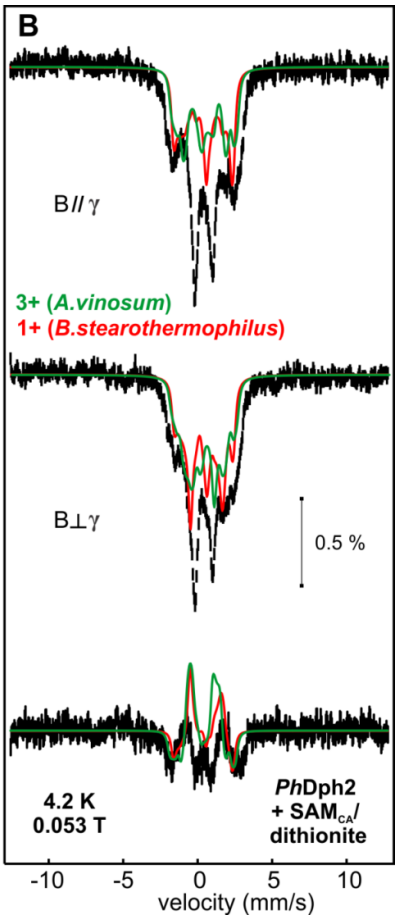

Figure S27: 4.2-K/53-mT spectra of the sample of the CA complex formed by incubation of AI *Ph*Dph2 with SAM_{CA} followed by treatment with excess dithionite for 9 minutes. The magnetic field is oriented parallel (top) or perpendicular (middle) to the propagation direction of the γ beam. The difference spectrum (parallel-minus-perpendicular) is shown on the bottom. Experimental data are shown as black vertical bars. The red and green solid lines are simulations using published parameters of the $[4Fe\text{-}4S]^{+}$ cluster of *Bacillus stearothermophilus* ferredoxin [mixed-valent site: $\delta = 0.50$ mm/s, $\Delta E_Q = +1.32$ mm/s, $\eta = 0.8$, **A** = (-31.7, -32.6, -27.9) MHz and diferrous site: $\delta = 0.58$ mm/s, $\Delta E_Q = +1.89$ mm/s, $\eta = 0.3$, **A** = (+26.5, +13.5, +8.6) MHz] and of the $[4Fe\text{-}4S]^{3+}$ cluster of *Allochromatium vinosum* high-potential iron protein [mixed-valent site: $\delta = 0.40$ mm/s, $\Delta E_Q = -1.03$ mm/s, $\eta = 0.9$, **A** = (-28.3, -30.6, -32.6) MHz and diferric site: $\delta = 0.29$ mm/s, $\Delta E_Q = -0.88$ mm/s, $\eta = 0.4$, **A** = (+19,2, +22.4, +19.3) MHz], respectively.

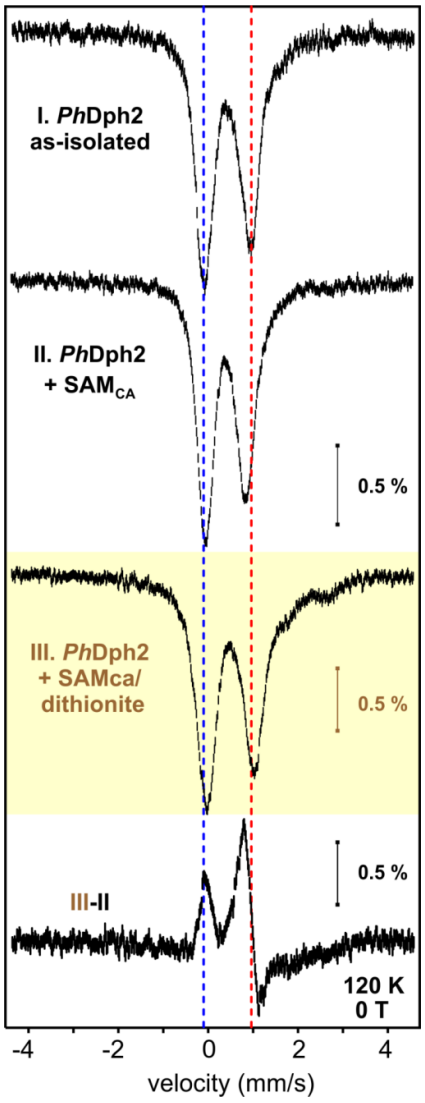

Figure S28: 120-K/zero-field Mössbauer spectra of anaerobically isolated (AI) *Ph*Dph2 (top), AI *Ph*Dph2 incubated with SAM_{CA} (middle), and of the CA complex formed by incubatioin of AI *Ph*Dph2 with SAM_{CA} followed by treatment with excess dithionite for 9 minutes (bottom). The blue and red dotted lines indicate the position of the low-energy and high-energy lines of the $[4Fe\text{-}4S]^{2+}$ cluster of as-isolated *Ph*Dph2, respectively.

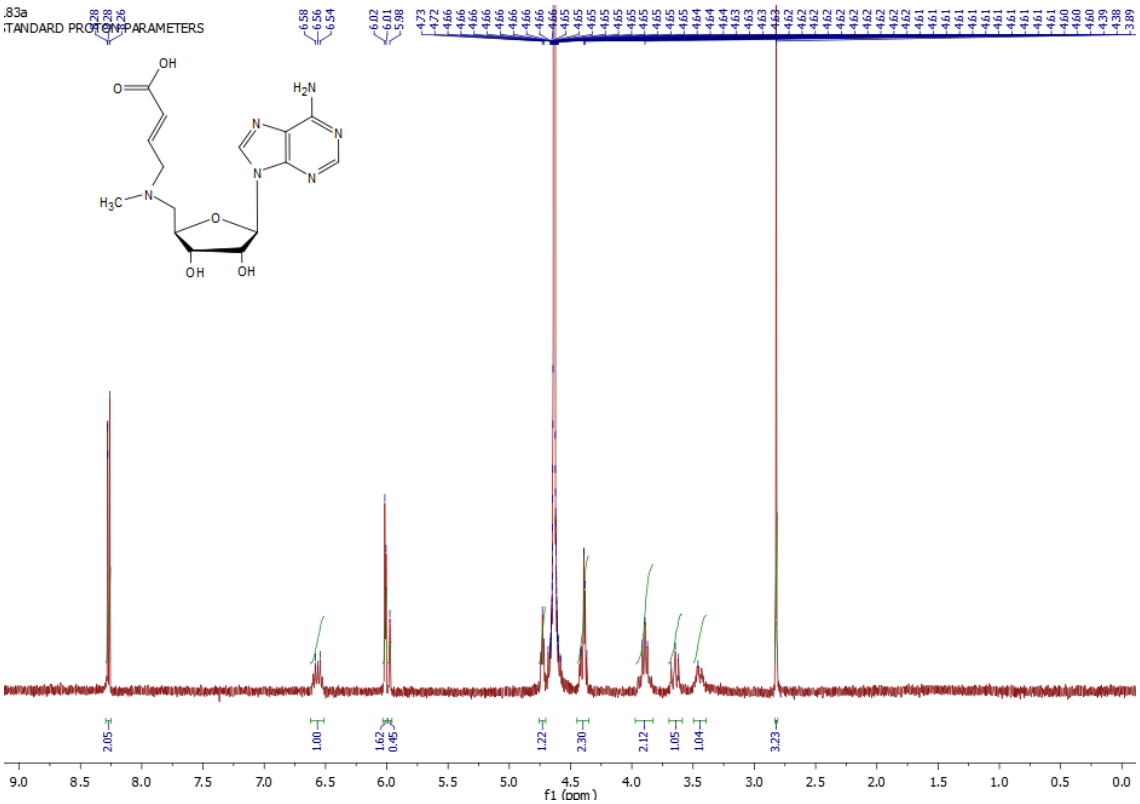

Figure S29. ^{1}H-NMR spectrum of aza-SAM$_{CA}$.

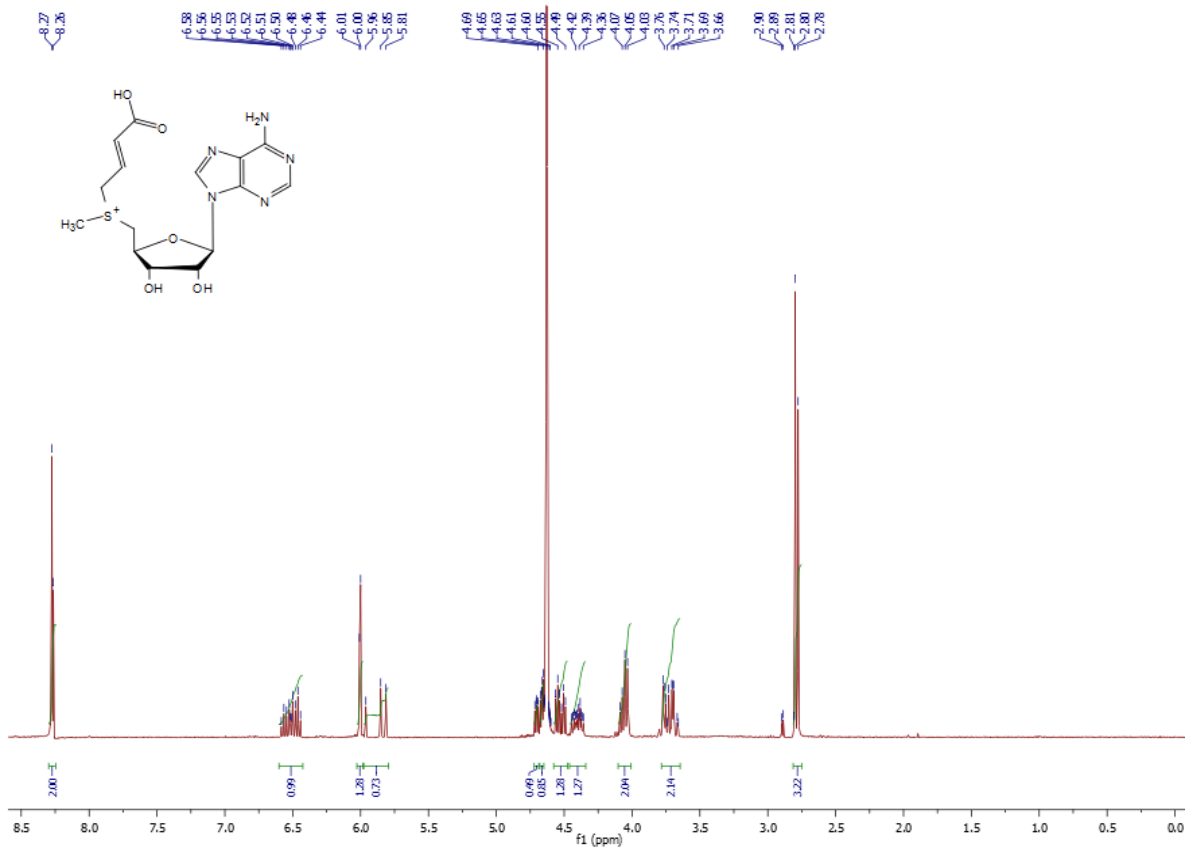

Figure S30. ^{1}H-NMR spectrum of SAM$_{CA}$.

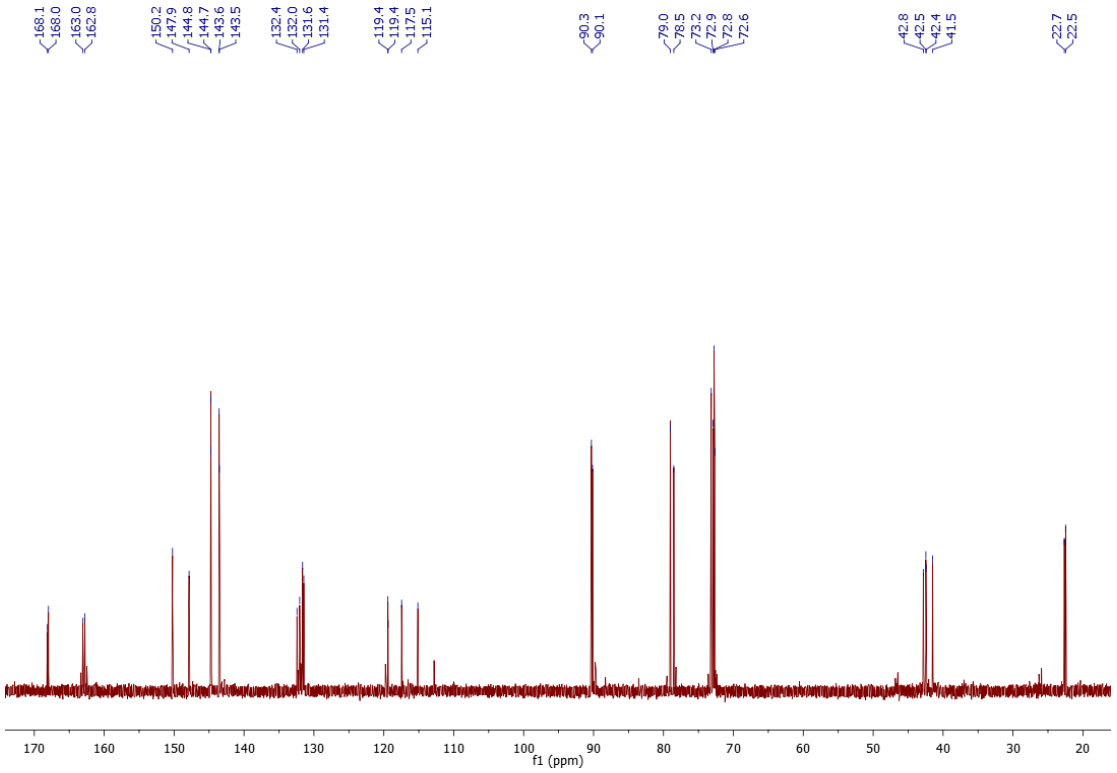

Figure S31. ^{13}C-NMR spectrum of SAM$_{CA}$

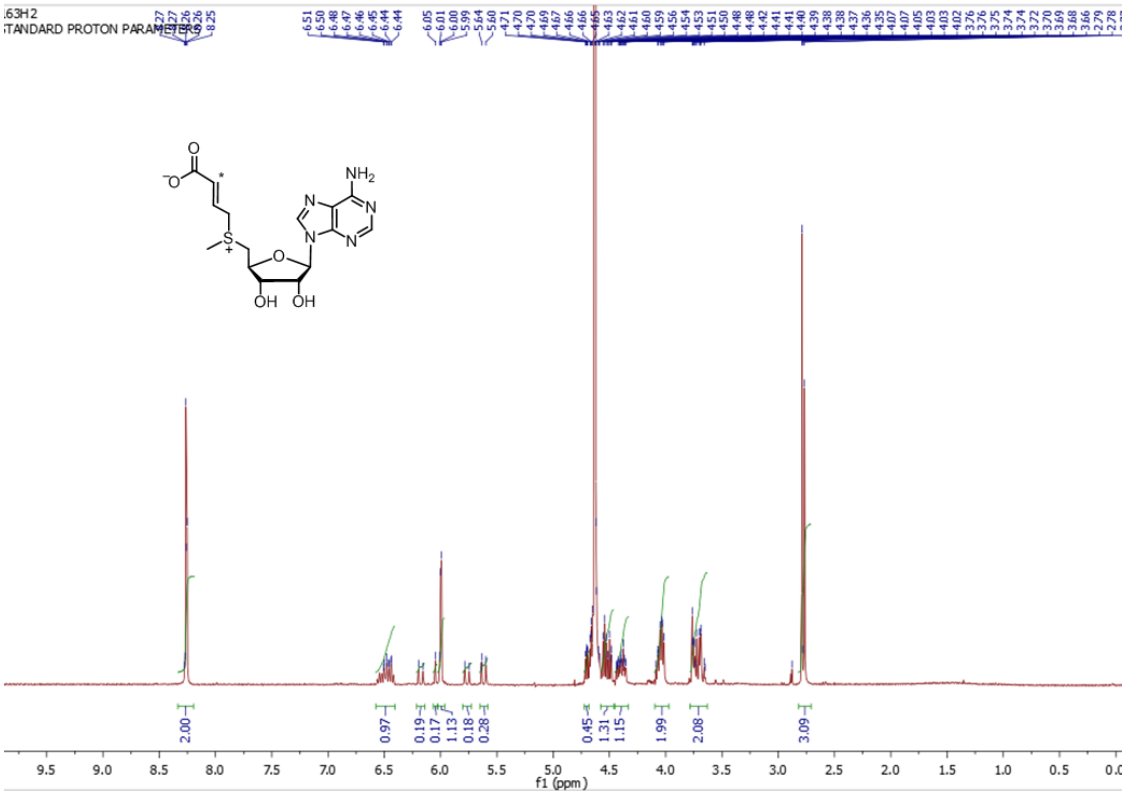

Figure S32. ^{1}H-NMR spectrum of 3-^{13}C SAM$_{CA}$.

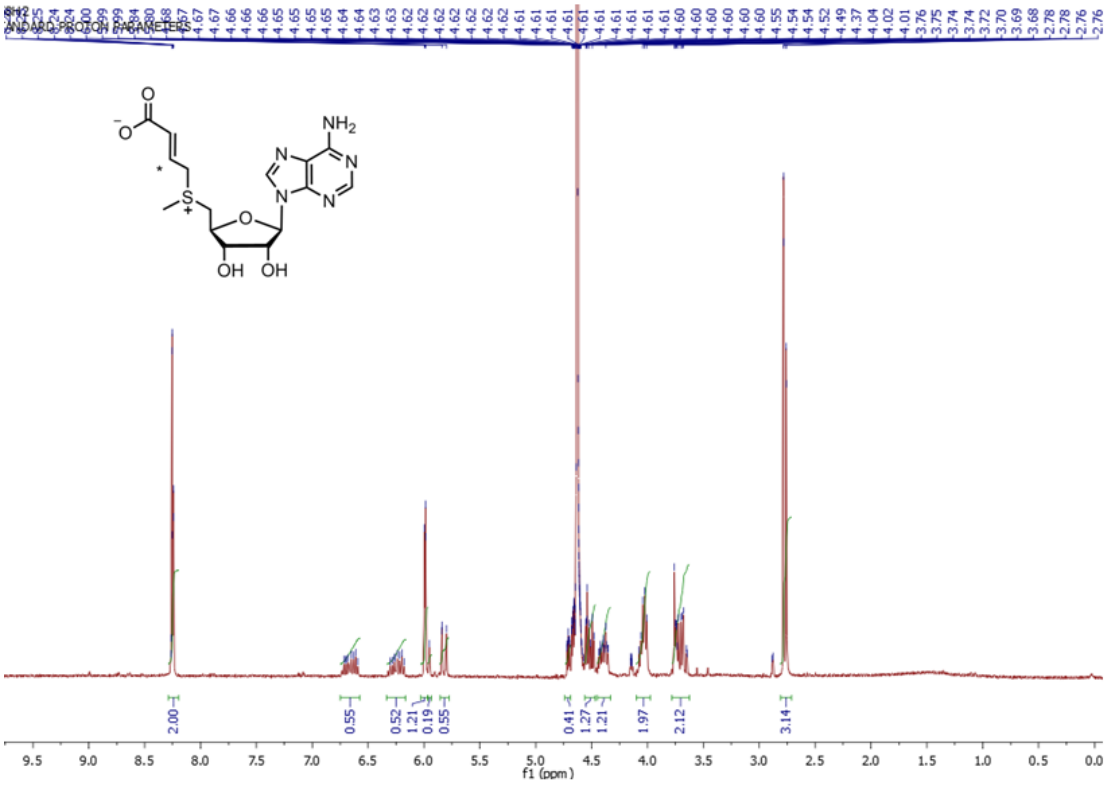

Figure S33. ^{1}H-NMR spectrum of 2-^{13}C SAM$_{CA}$

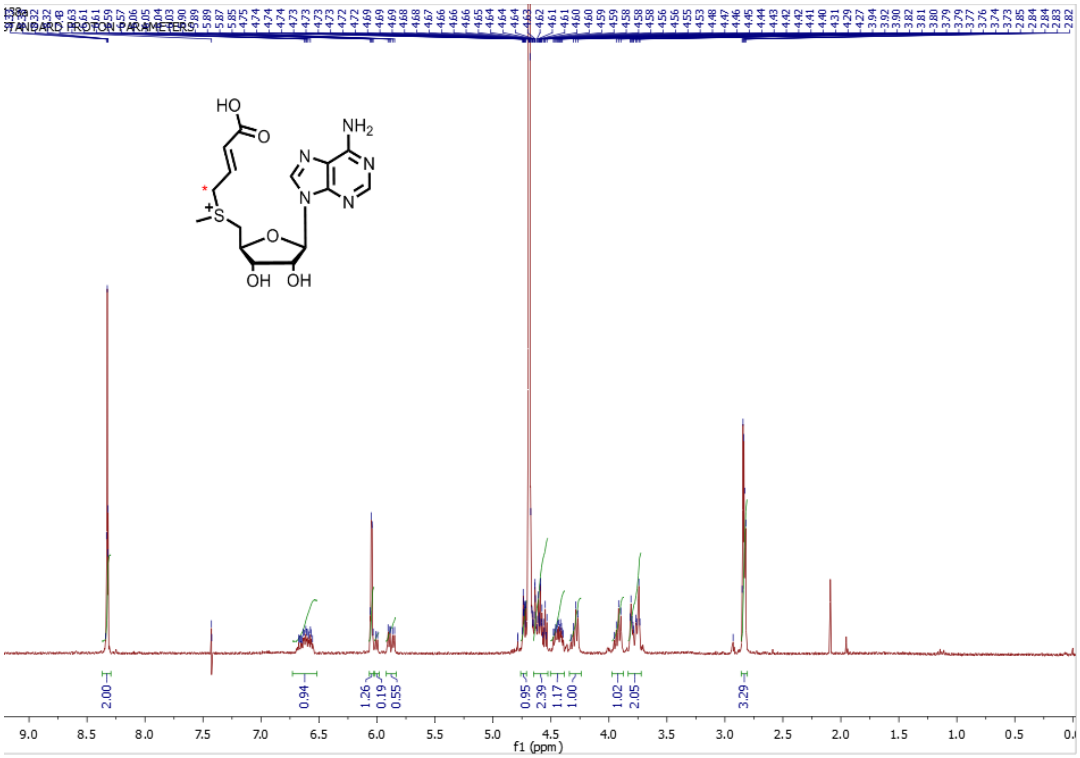

Figure S34. ^{1}H-NMR spectrum of 1-^{13}C SAM$_{CA}$

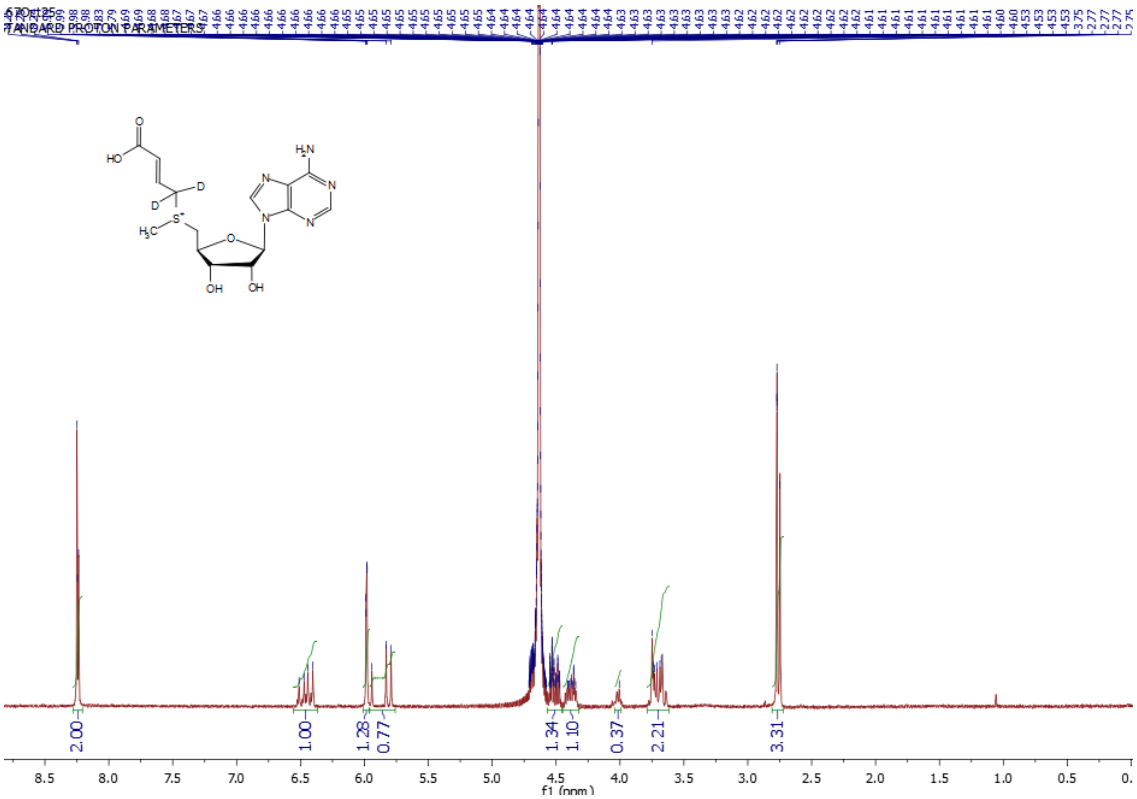

Figure S35. ^{1}H-NMR spectrum of 1,1-$^{2}H_2$ SAM$_{CA}$

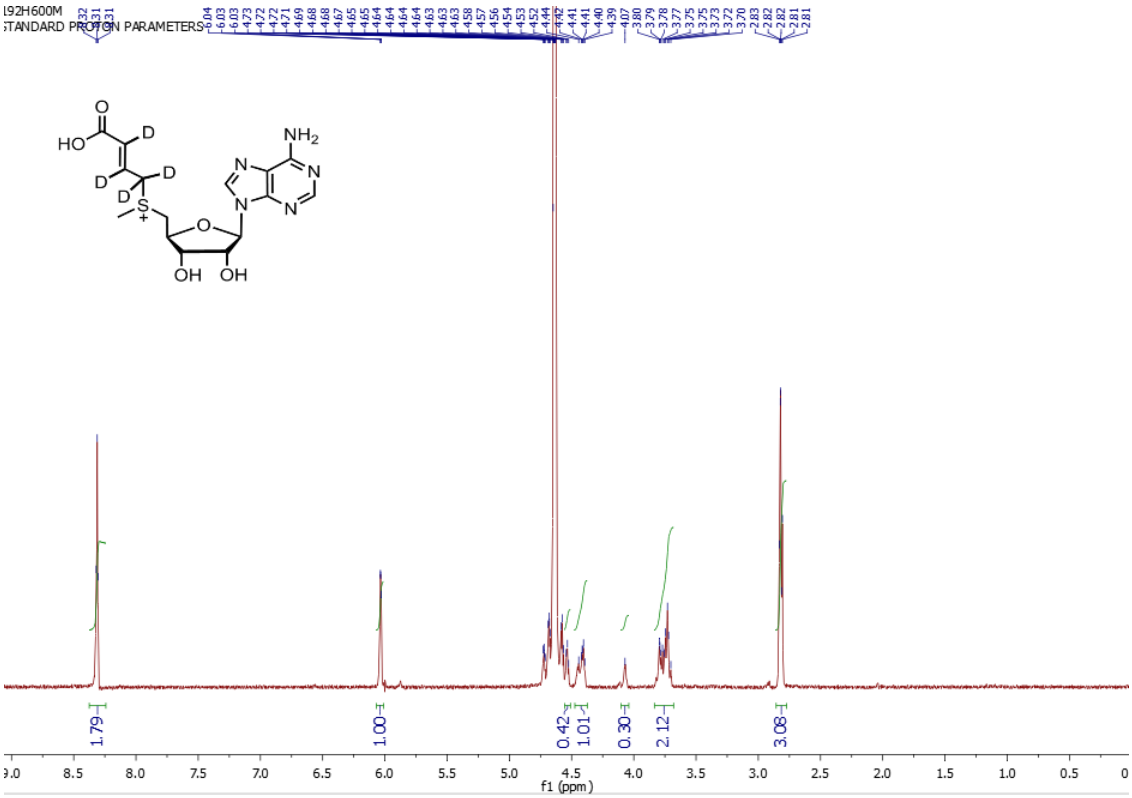

Figure S36. ^{1}H-NMR spectrum of 1,1,2,3-$^{2}H_4$ SAM$_{CA}$

C. References

(1) Werst, M. M.; Davoust, C. E.; Hoffman, B. M. *J.Am. Chem. Soc* **1991**, *113*, 1533.

(2) Davoust, C. E. D., P. E.; Hoffman, B. M. *J.Magn.Reson* **1996**, *119*, 38.

(3) Wang, R.; Zheng, W.; Yu, H.; Deng, H.; Luo, M. *J. Am. Chem. Soc.* **2011**, *133*, 7648.

(4) Zhang, Y.; Zhu, X.; Torelli, A. T.; Lee, M.; Dzikovski, B.; Koralewski, R. M.; Wang, E.; Freed, J.; Krebs, C.; Ealick, S. E.; Lin, H. *Nature* **2010**, *465*, 891.

(5) Wong, C. H.; Whitesides, G. M. *J.Am.Chem.Soc.* **1983**, *105*, 5012.

(6) Doan, P. E.; Hoffman, B. M. *Chemical Physics Letters* **1997**, *269*, 208.

(7) Clark, J. H.; Miller, J. M. *Tetrahedron. Letters.* **1977**, *18*, 599.

(8) Broderick, J. B.; Duffus, B. R.; Duschene, K. S.; Shepard, E. M. *Chemical. Reviews.* **2014**, *114*, 4229.

(9) Beinert, H.; Kennedy, M. C.; Stout, C. D. *Chemical. Reviews* **1996**, *96*, 2335.

(10) Khatik, G. L.; Kumar, R.; Chakraborti, A. K. *Org.Lett.* **2006**, *8*, 2433.